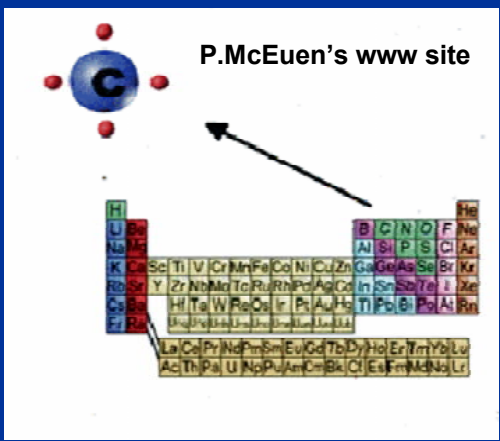
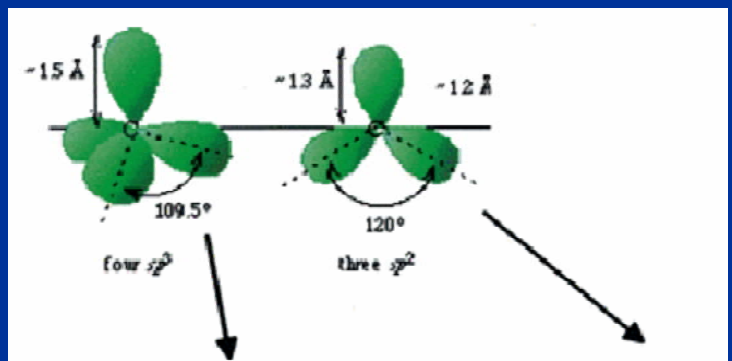


# Introduction

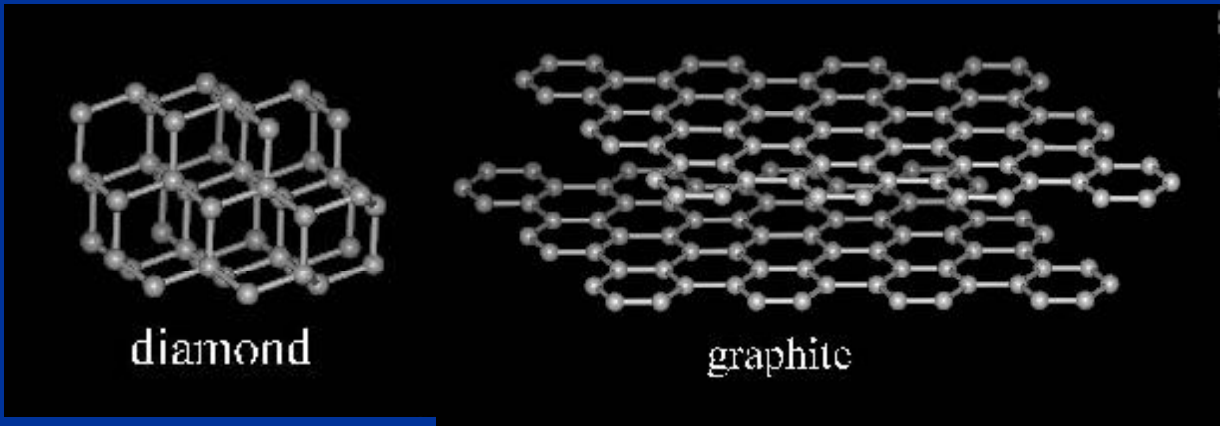
## Nanotubes and Nanodevices

# C - New Material for Electronics?

4 valence electrons/at.  $sp^3$  and  $sp^2$  hybridization



Allotrope modifications for  $sp^2$ -carbon - planar:  
• graphites



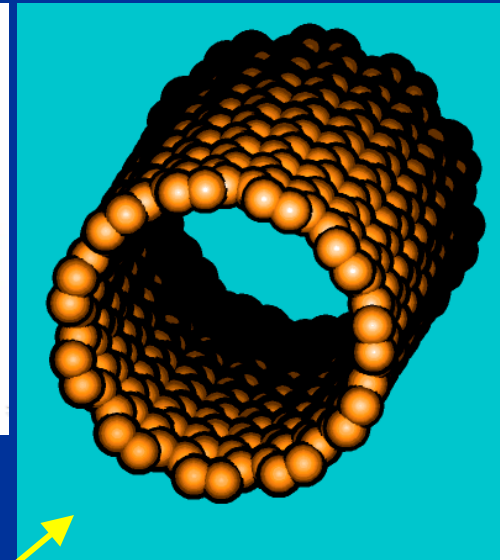
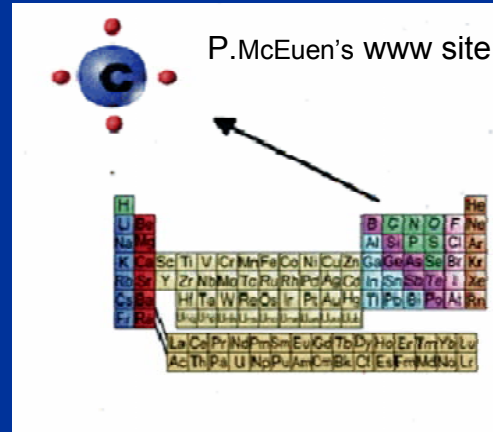
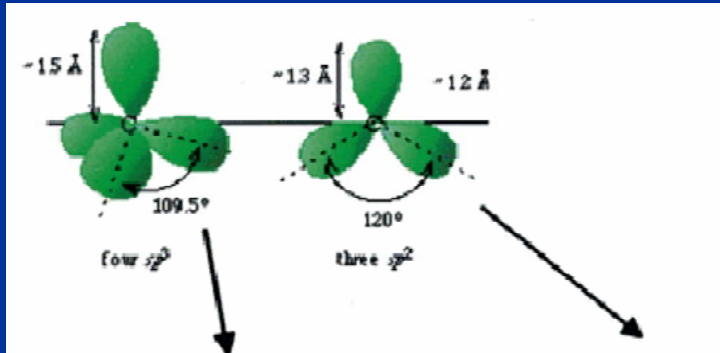


APS has selected Dr. **Sumio Iijima** and Dr. **Donald S. Bethune** to receive in 2002 James C. McGroddy Prize for New Materials

**"For the discovery and development of single-wall carbon nanotubes, which can behave like metals or semiconductors, can conduct electricity better than copper, can transmit heat better than diamond, and rank among the strongest materials known."**

# C - New Material for Electronics

4 valence electrons/at.  $sp^3$  and  $sp^2$  hybridization

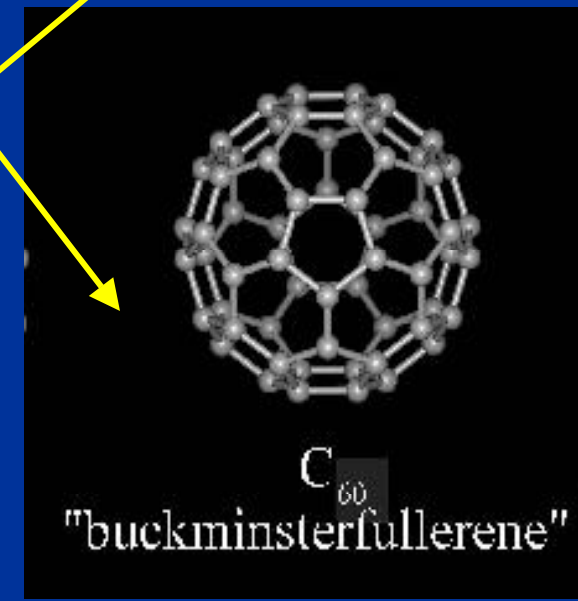
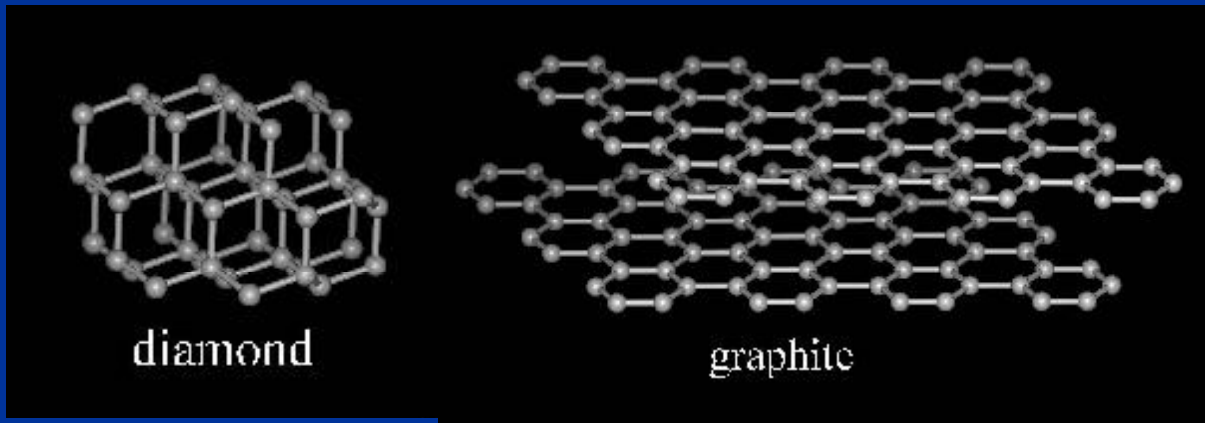


Allotrope modifications for  $sp^2$ -carbon - planar:

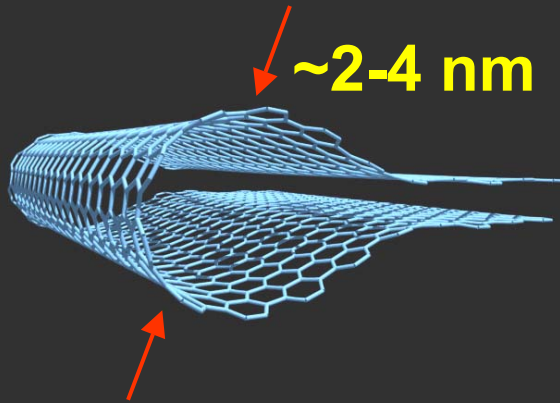
- graphites

- embedded into curved space:

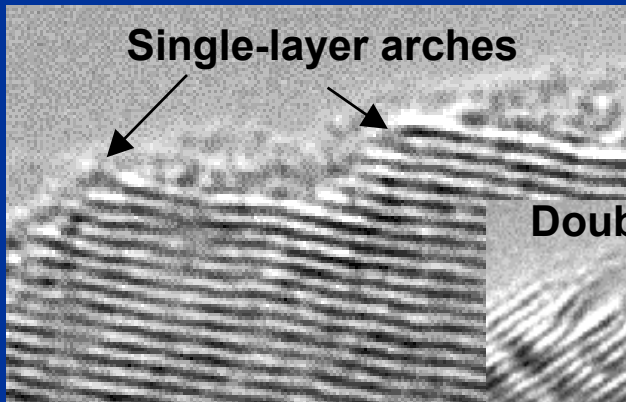
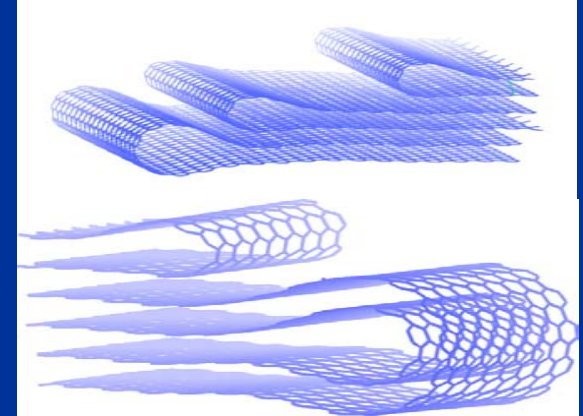
- fullerenes
- nanotubes



# Scrolling at the Nanoscale



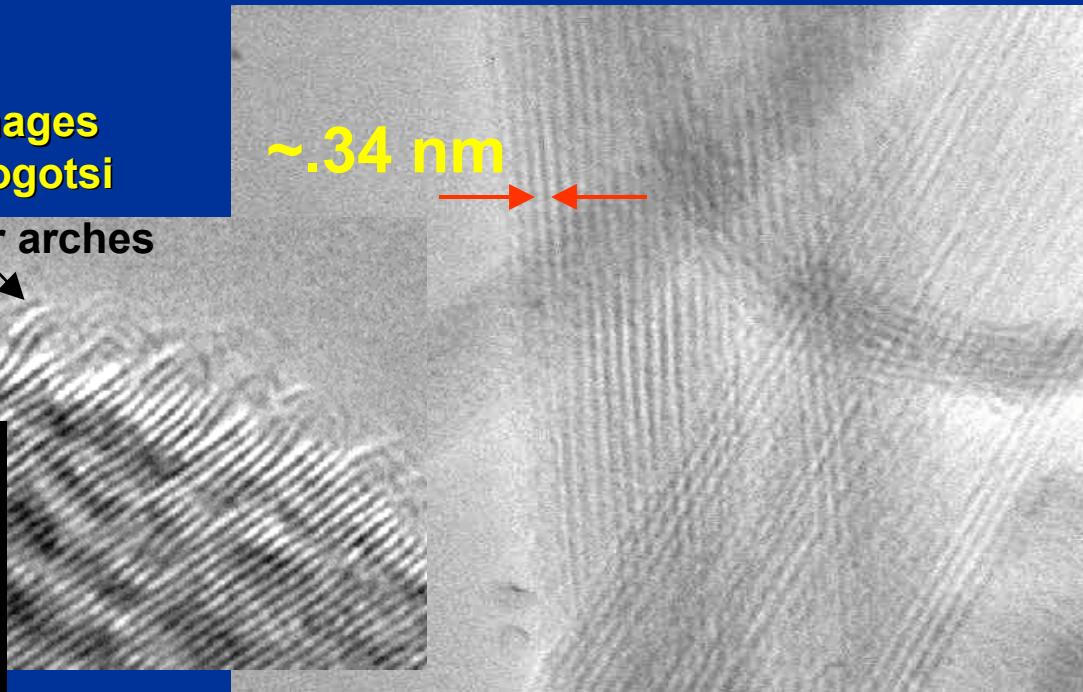
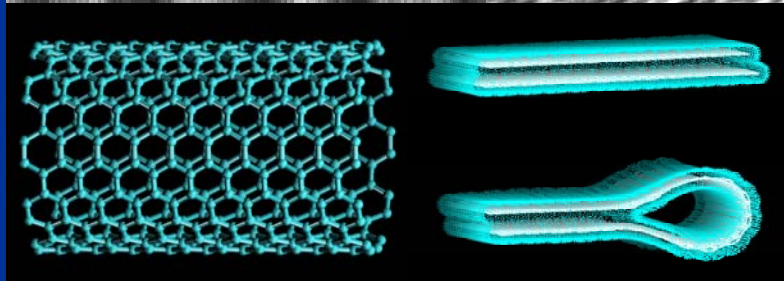
Material properties of the layered lattice of the graphite define an internal nanoscale at which a process of the scrolling happens.



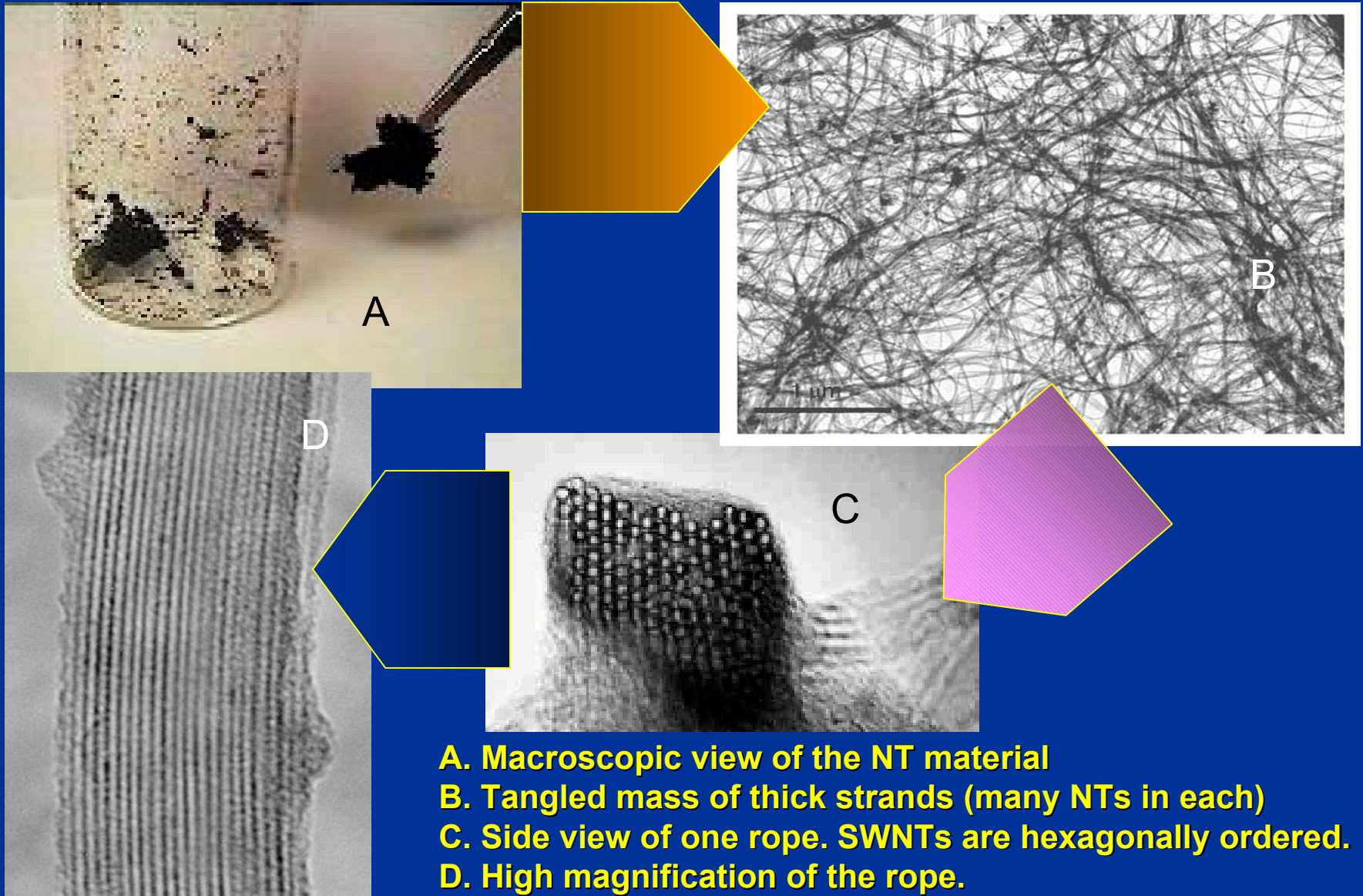
TEM images by Y.Gogotsi



~.34 nm

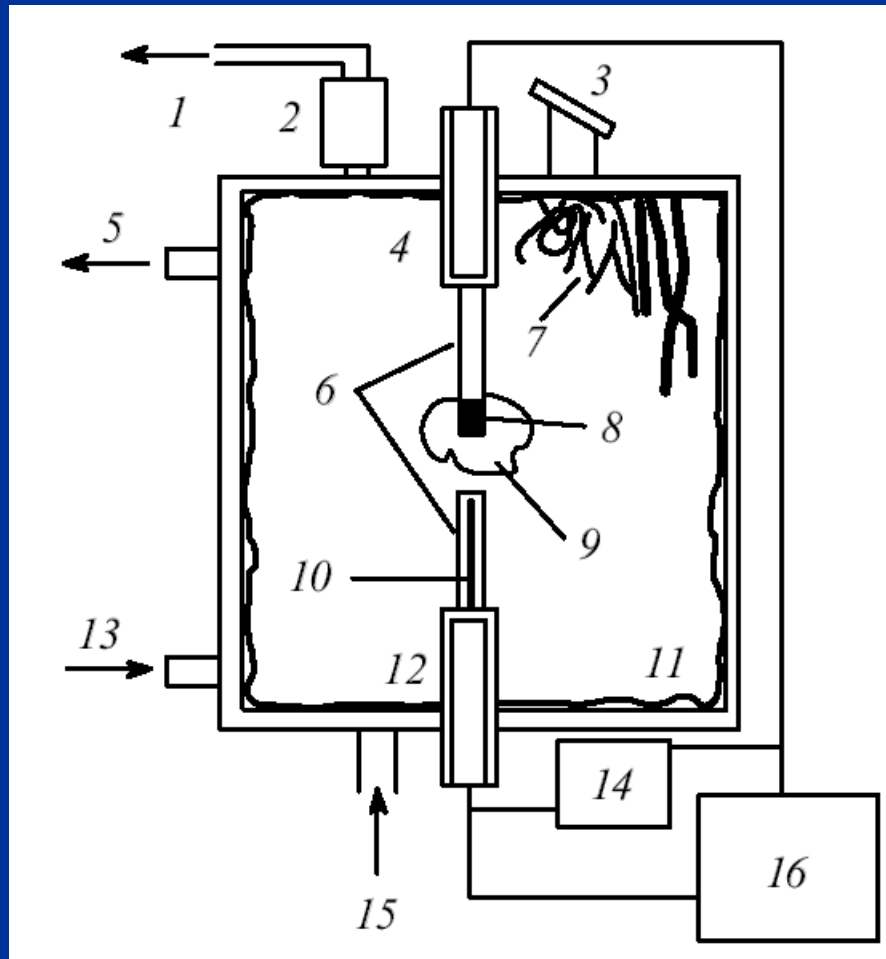


# NT Material: What is it?

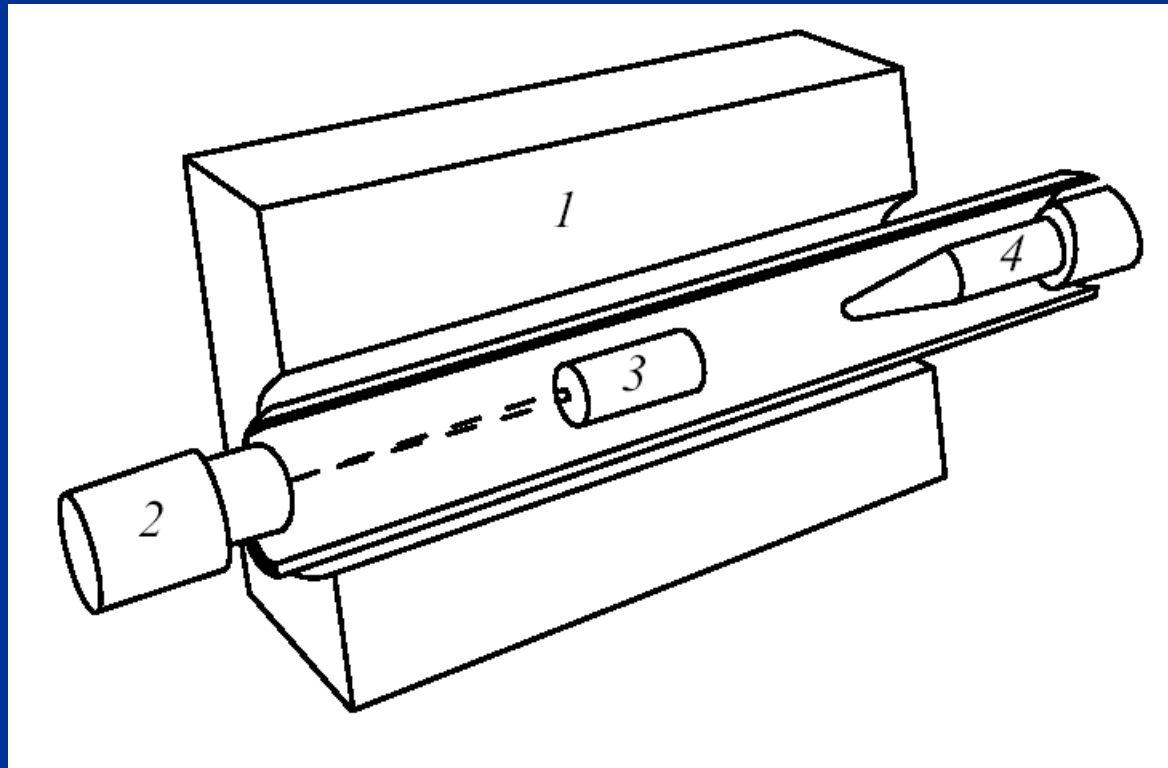


- A. Macroscopic view of the NT material**
- B. Tangled mass of thick strands (many NTs in each)**
- C. Side view of one rope. SWNTs are hexagonally ordered.**
- D. High magnification of the rope.**

# Production: Arc technique

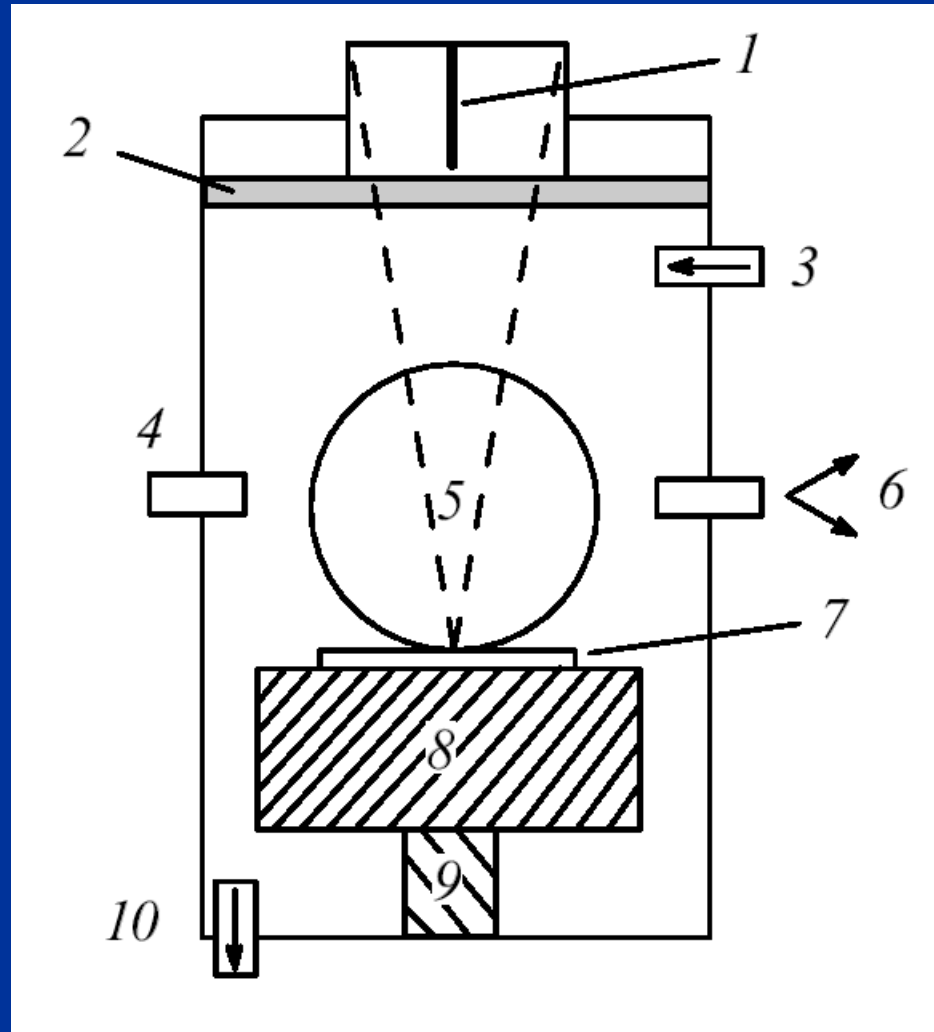


# Production: Laser vaporization





# Production: PCVD technique

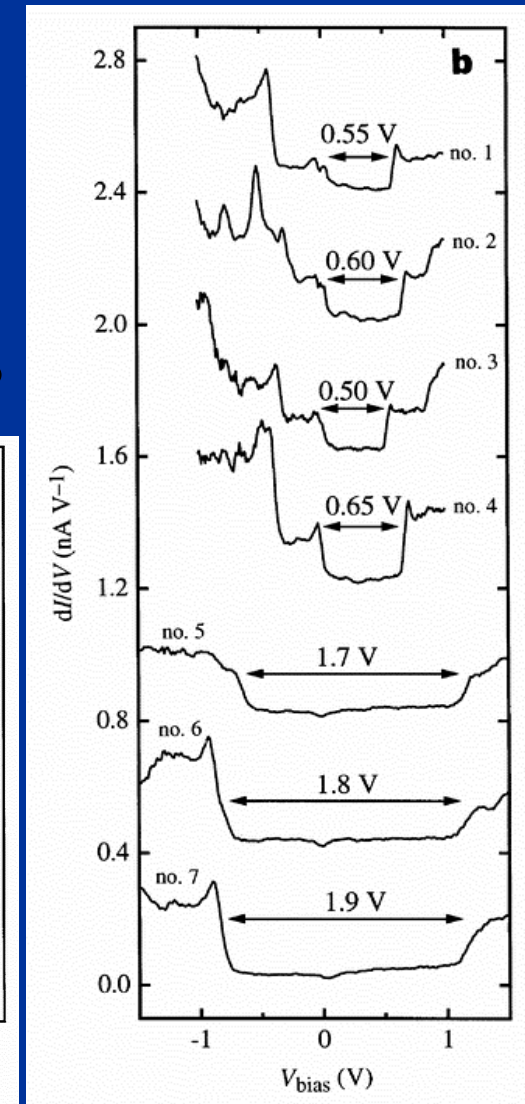
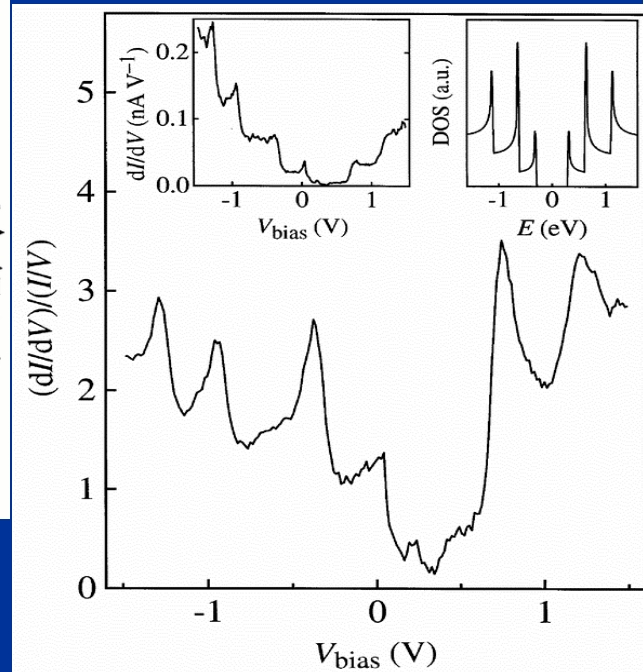
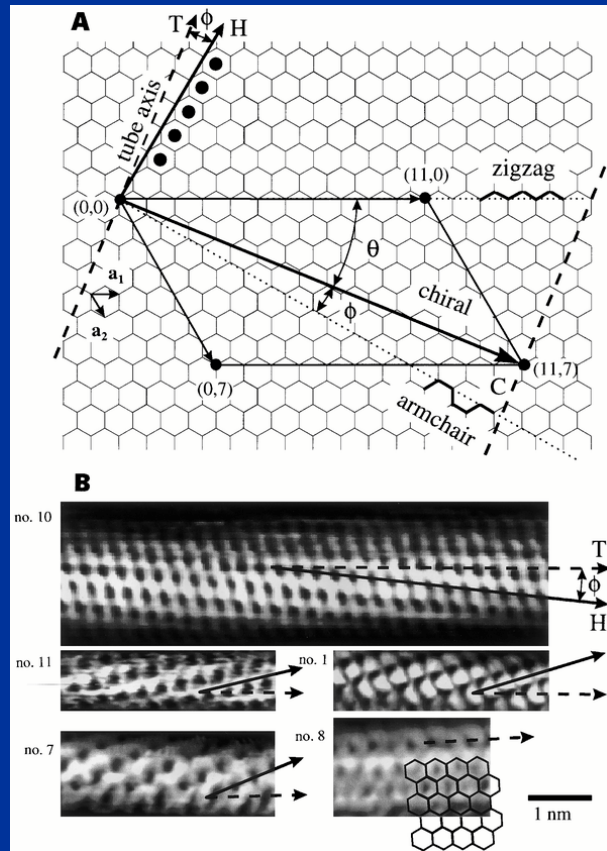


# DOS of SWNT: STS

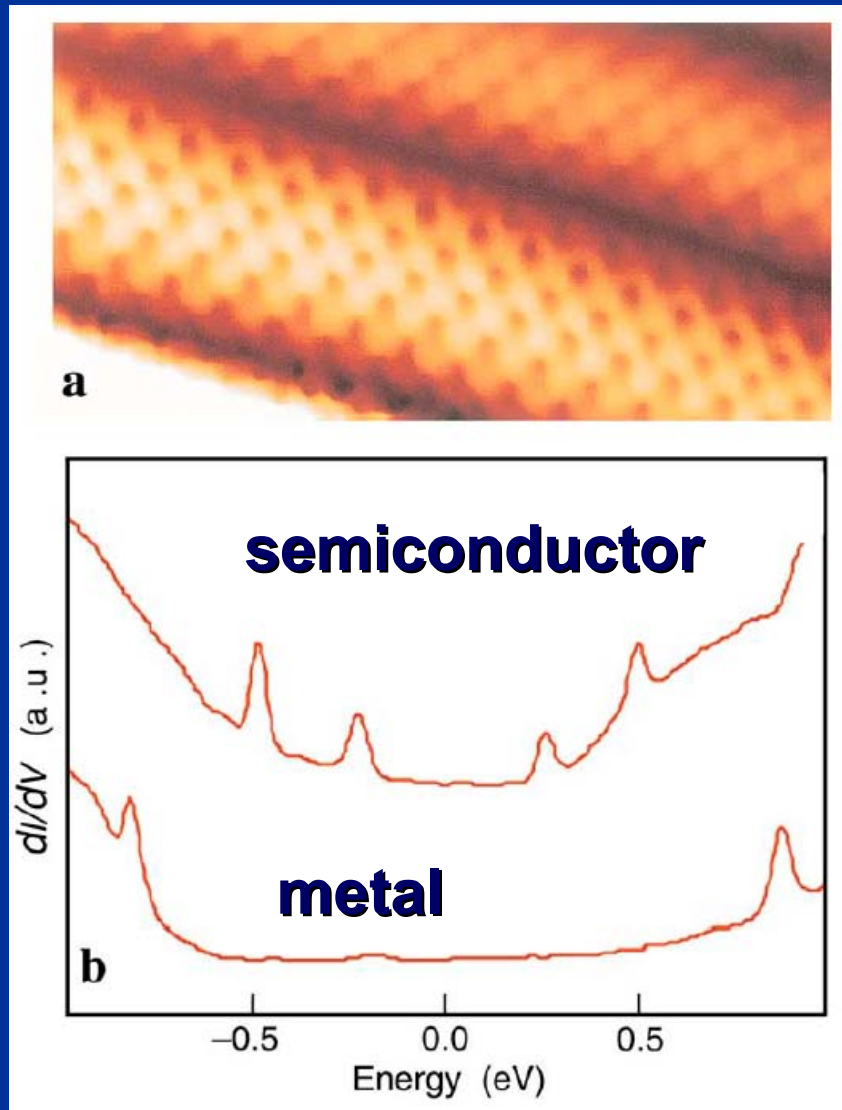
C. Dekker group (1998)

## Graphite scrolling

- 2 types of STS gap
- pinning of  $E_F$  in Se-SWNT to  $E_V$
- zero-bias dip
- STS reflects 1D-DOS



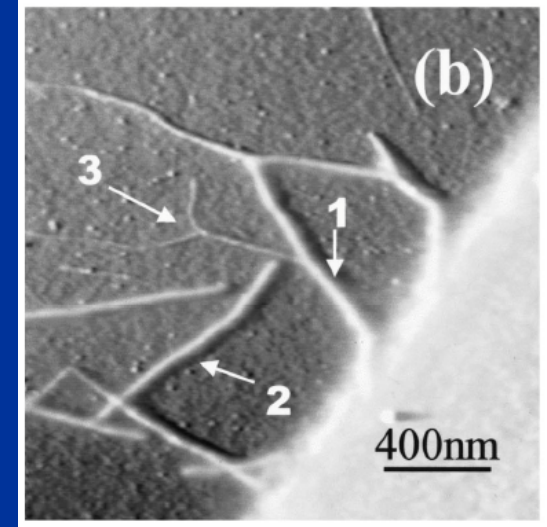
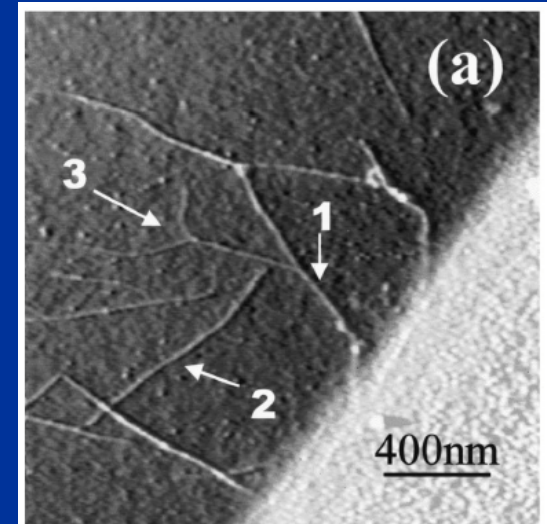
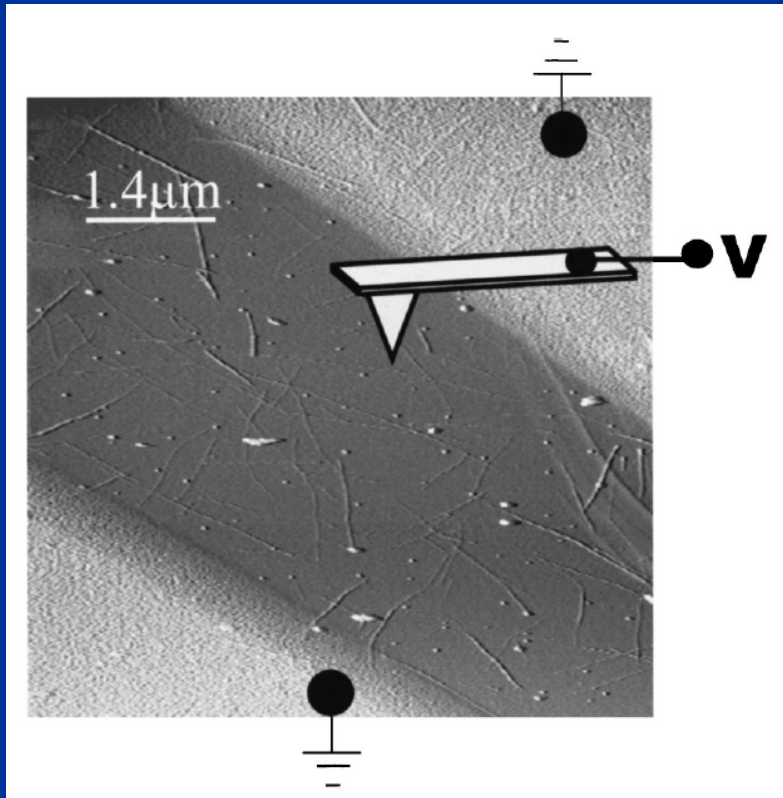
# DOS of SWNT: STS (2)



Adapted from Ch.Lieber and H.Dai

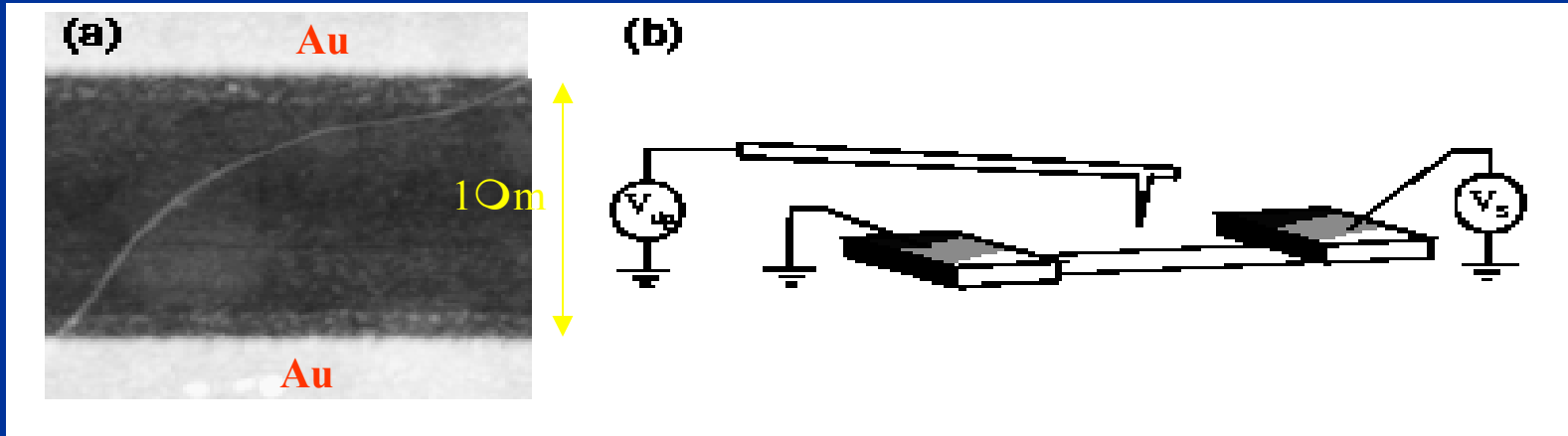
# Scanning Probe Technique

P. J. de Pablo (2001)



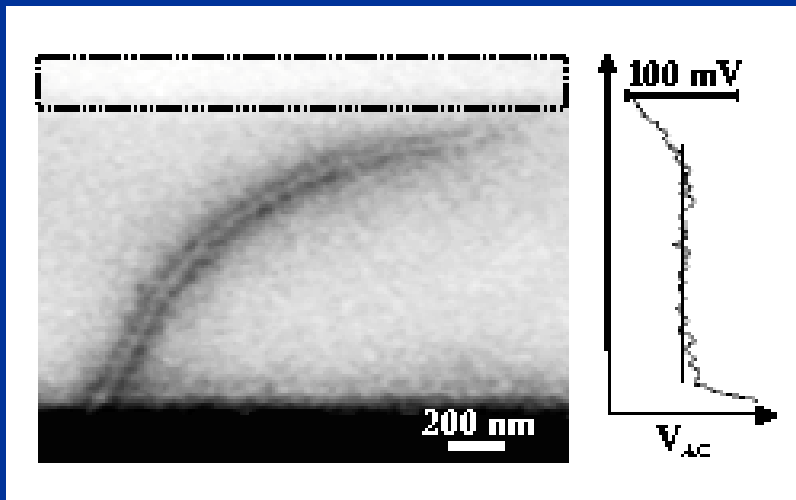
Additional resolution of SWNT was achieved with a conducting AFM cantilever scanned above the electrodes.

# Me SWNT: ballistic transport



(a) Topographic AFM image of a 2.5 nm diameter bundle of SWNTs

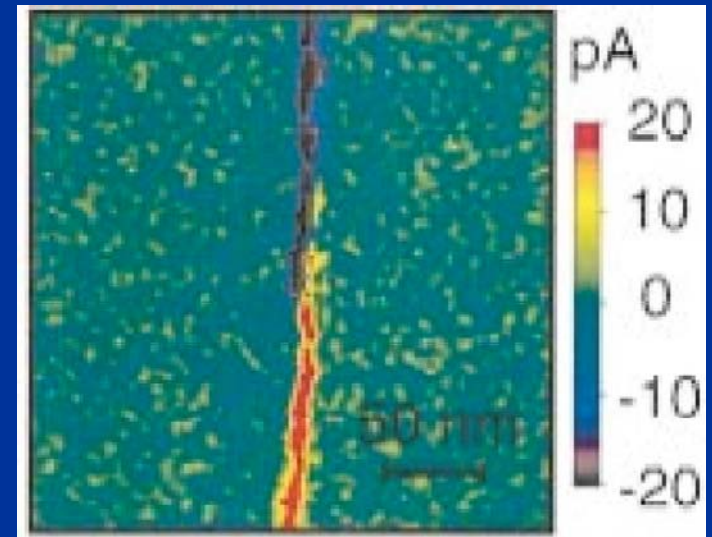
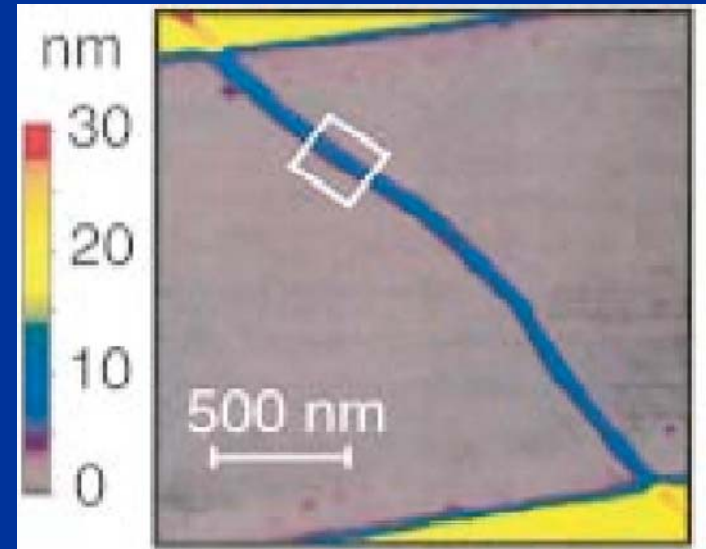
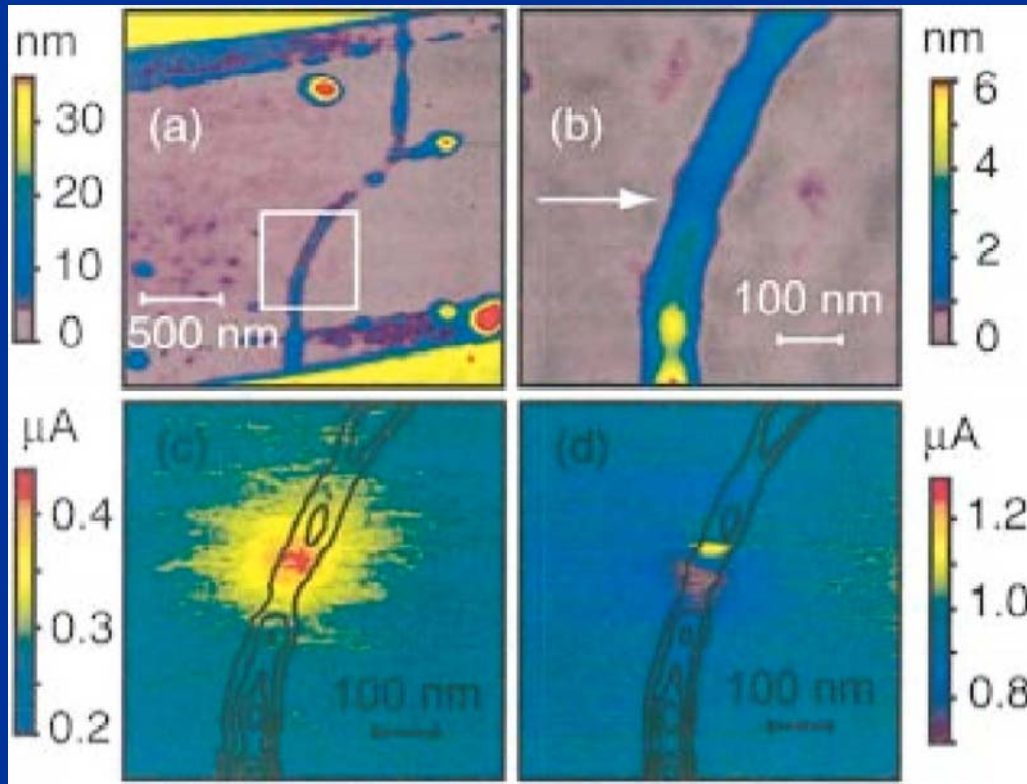
(b) Experimental setup for EFM. A conducting AFM cantilever is scanned above the device



McEuen Phys. Rev. Lett. (2000)

EFM image of the same bundle. An AC potential of 100 mV is applied to the lower electrode. The upper electrode indicated by box is grounded. AC-EFM signal is flat along the length of the SWNT bundle, indicating that the potential drops occur at contacts, and not along the bundle length. A trace of potential as function of vertical position in image is also shown.

# NT rope resistivity



A. T. Johnson Phys Rev B 2000

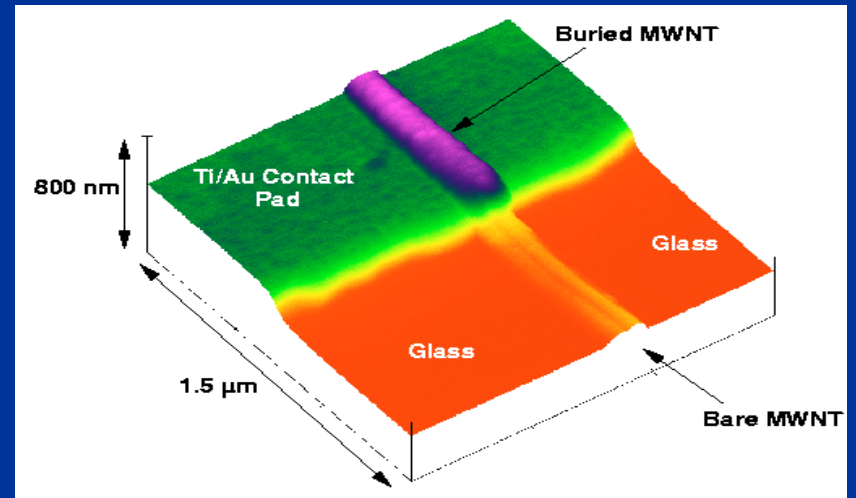
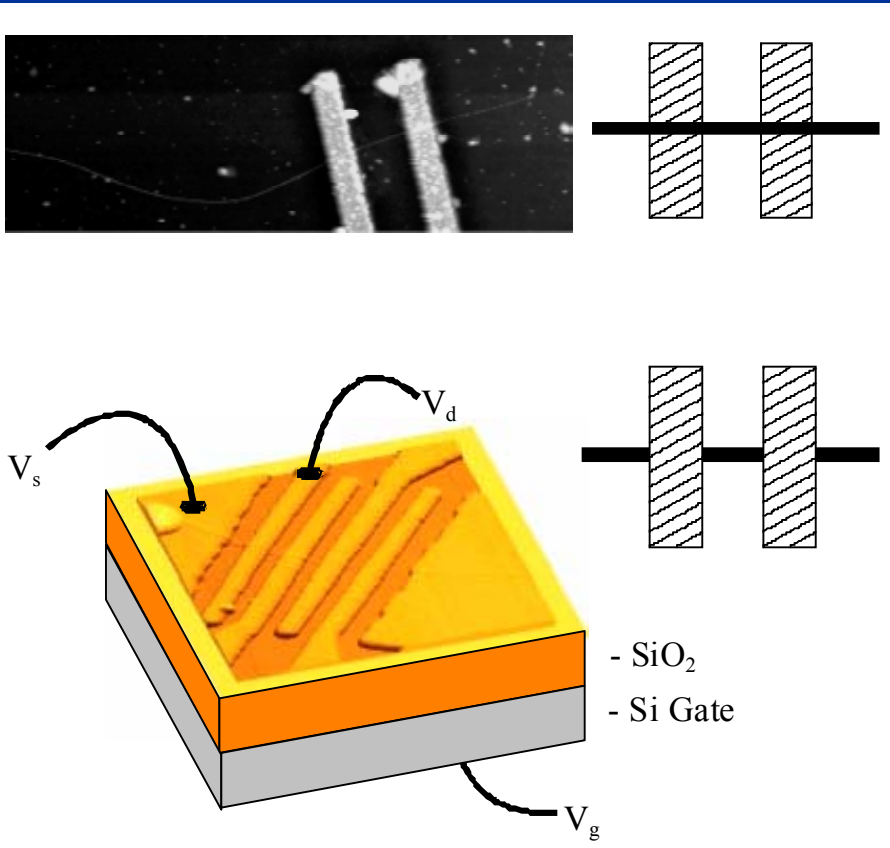
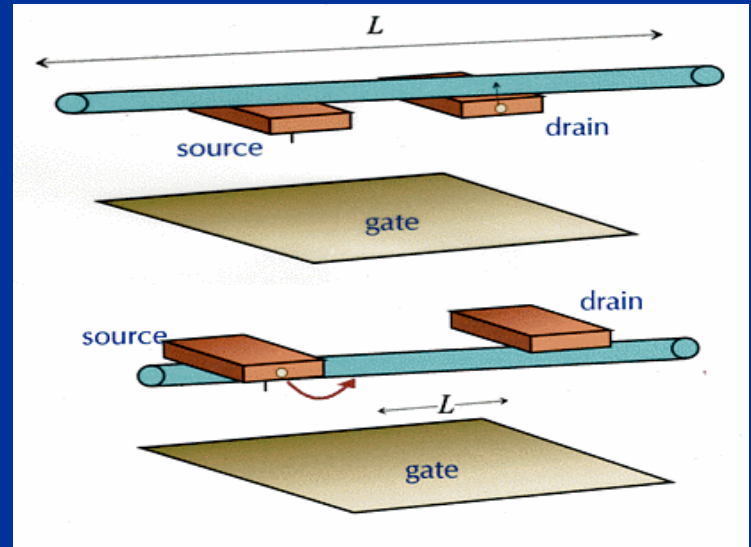
Local gate (AFM-C tip) probes potential drop along NT rope. Bad contact shows up as the potential relief.

# NT Device: Contacts

Tube on top: lighter interference but worse contact  
 Tube underneath: *vice versa*

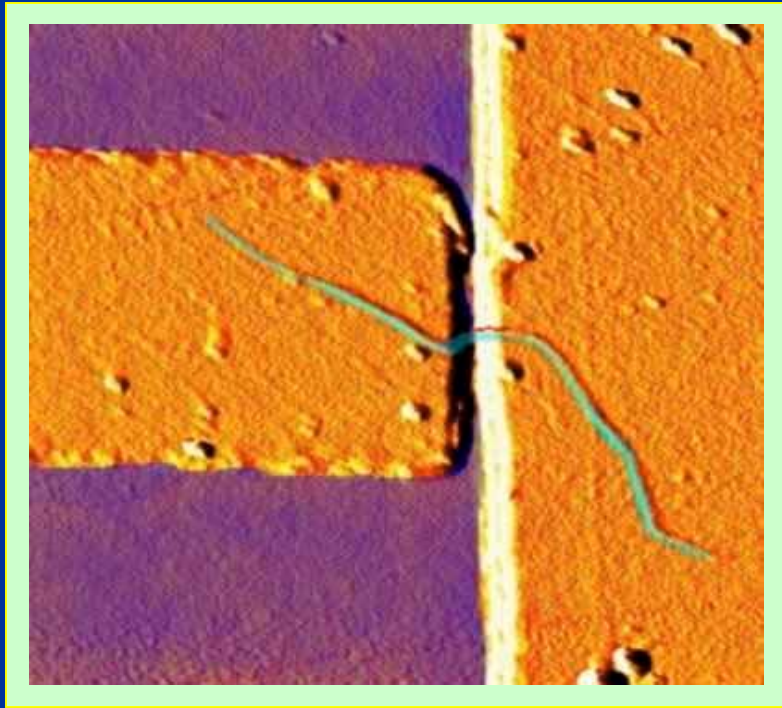
After P. McEuen

Tunneling:  $R_c \sim \text{tens } k\phi - G\phi$

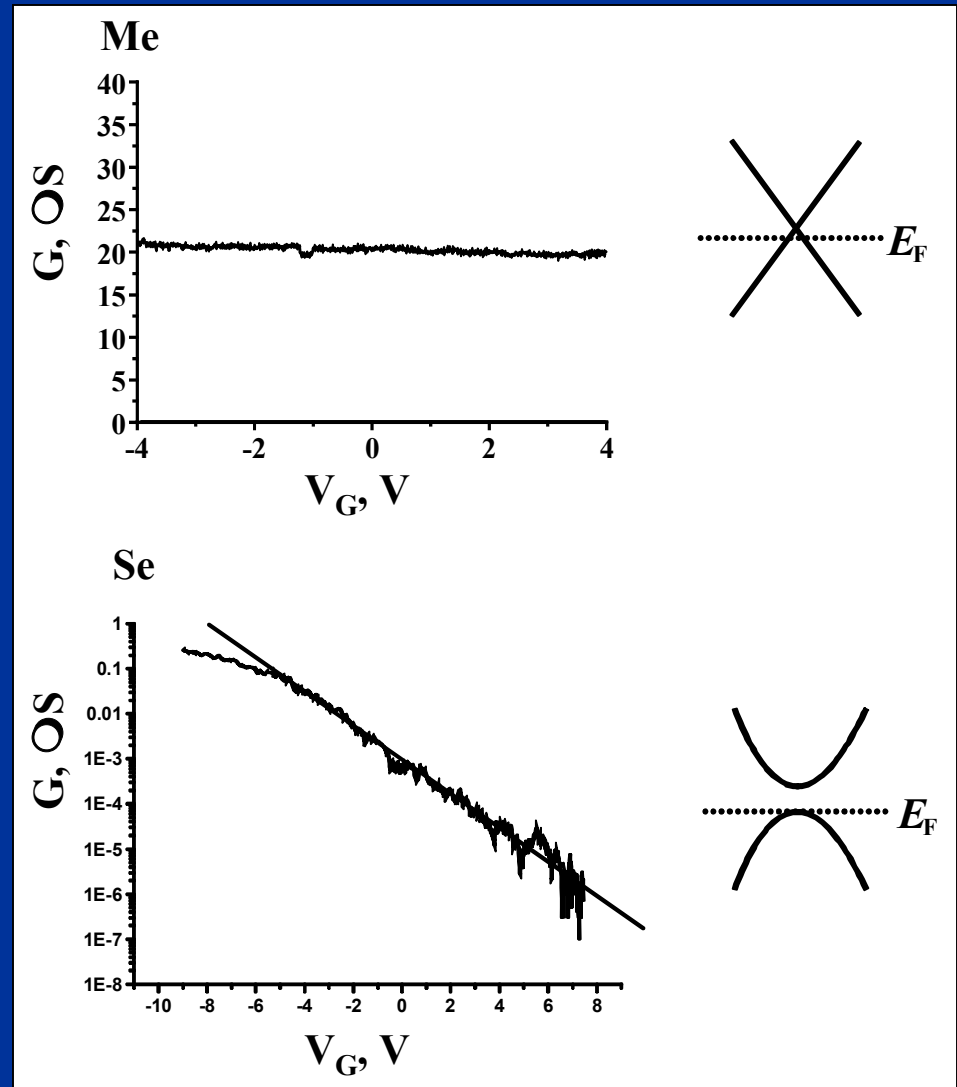


# SWNT Field Effect Devices

P. McEuen (1999)

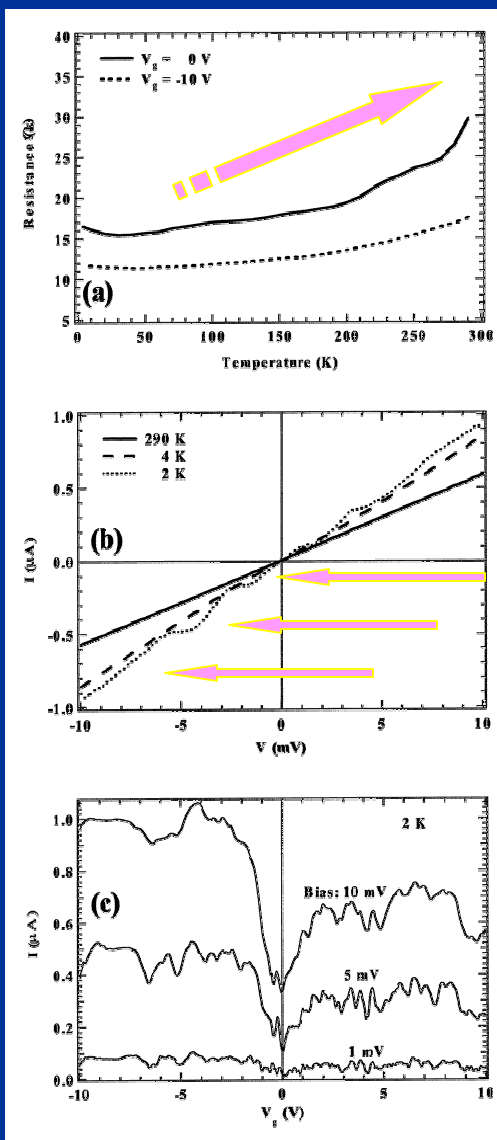


Gating has small effect on Me-SWNT conductivity but changes exponentially Se-SWNT conductivity

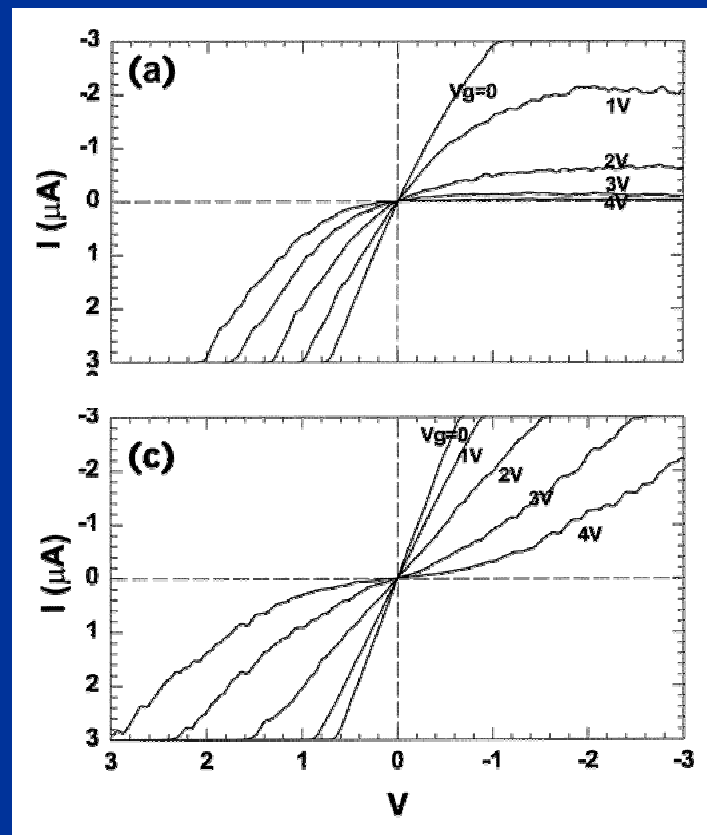




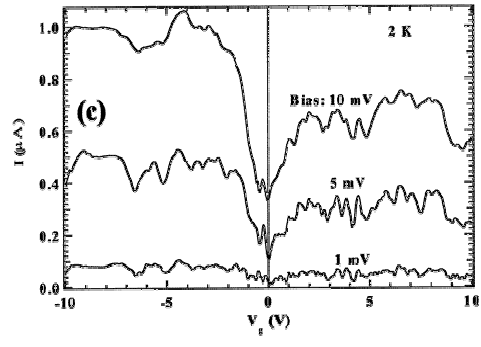
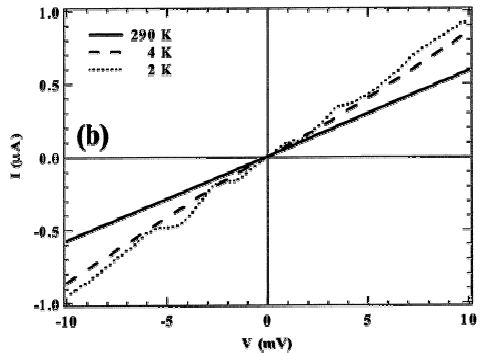
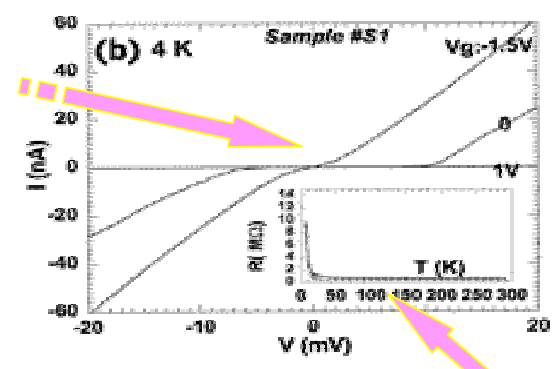
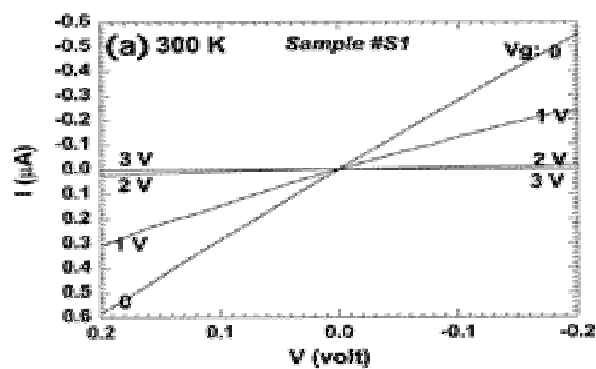
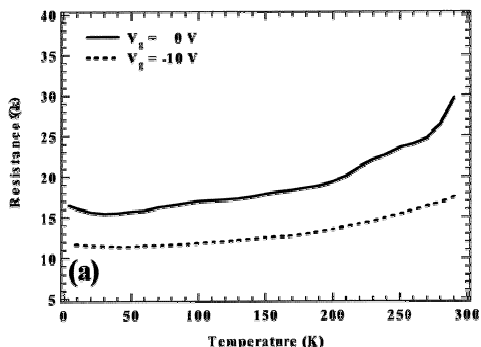
# Me & Se SWNTs



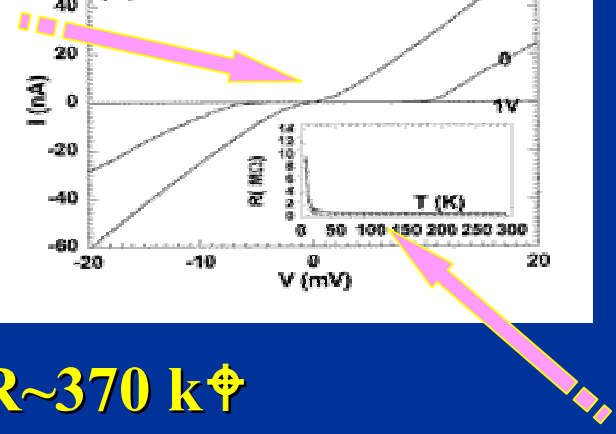
- R vs T shows Me behavior
- Ohm law transforms into DOS steps at low T
- Conductance depends on  $V_g$  but moderately
- Positive gate  $V_g^+$  suppress current
- I/V curve is not symmetrical for Se SWNT due to strong bias field
- for symmetrical bias both contacts show gating effect



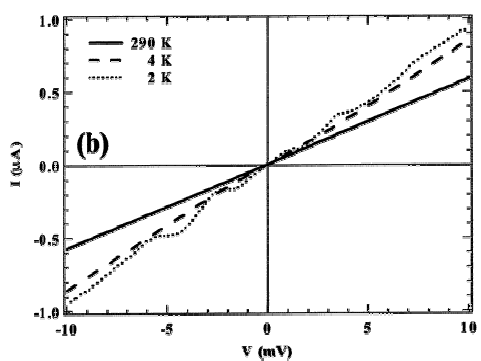
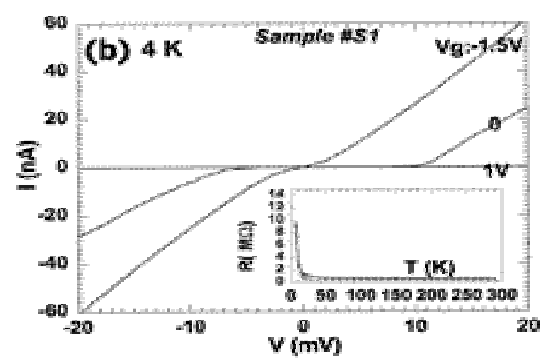
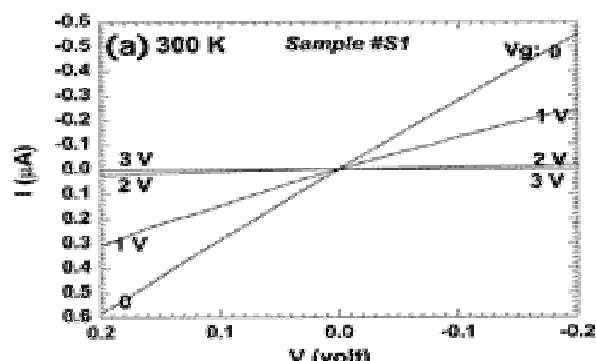
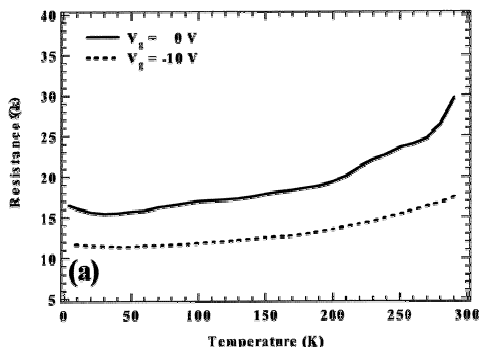
# Me & Se SWNTs



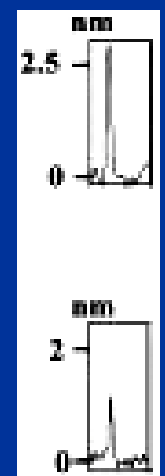
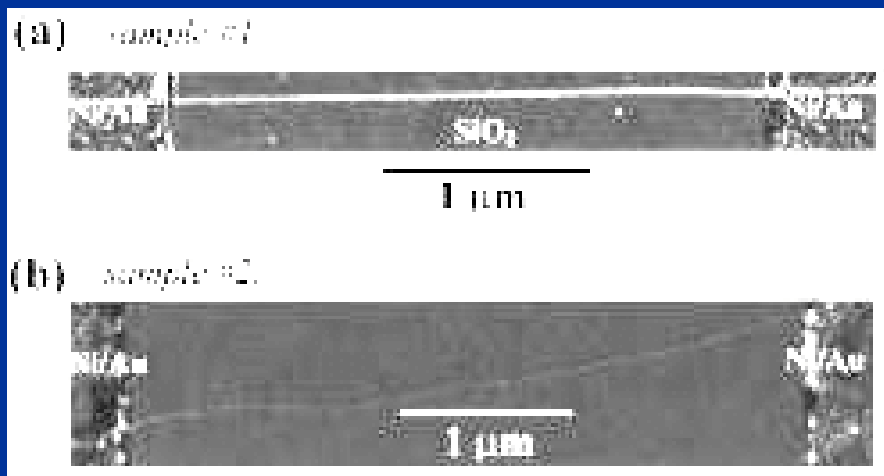
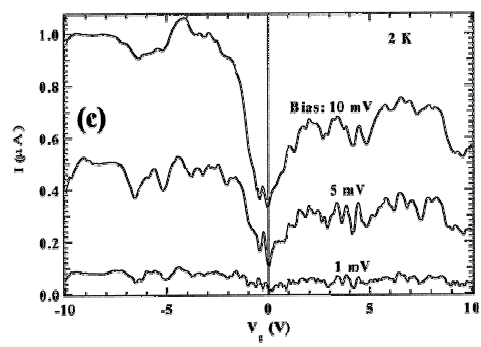
- $d \sim 2.8 \text{ nm}$ ,  $L \sim 3 \text{ } \mu\text{m}$ ,  $R \sim 370 \text{ k}\Omega$
- $\sim 20 \text{ mV}$  gap in  $I/V$  at helium
- below 25K activation barrier  $\sim 5 \text{ meV}$



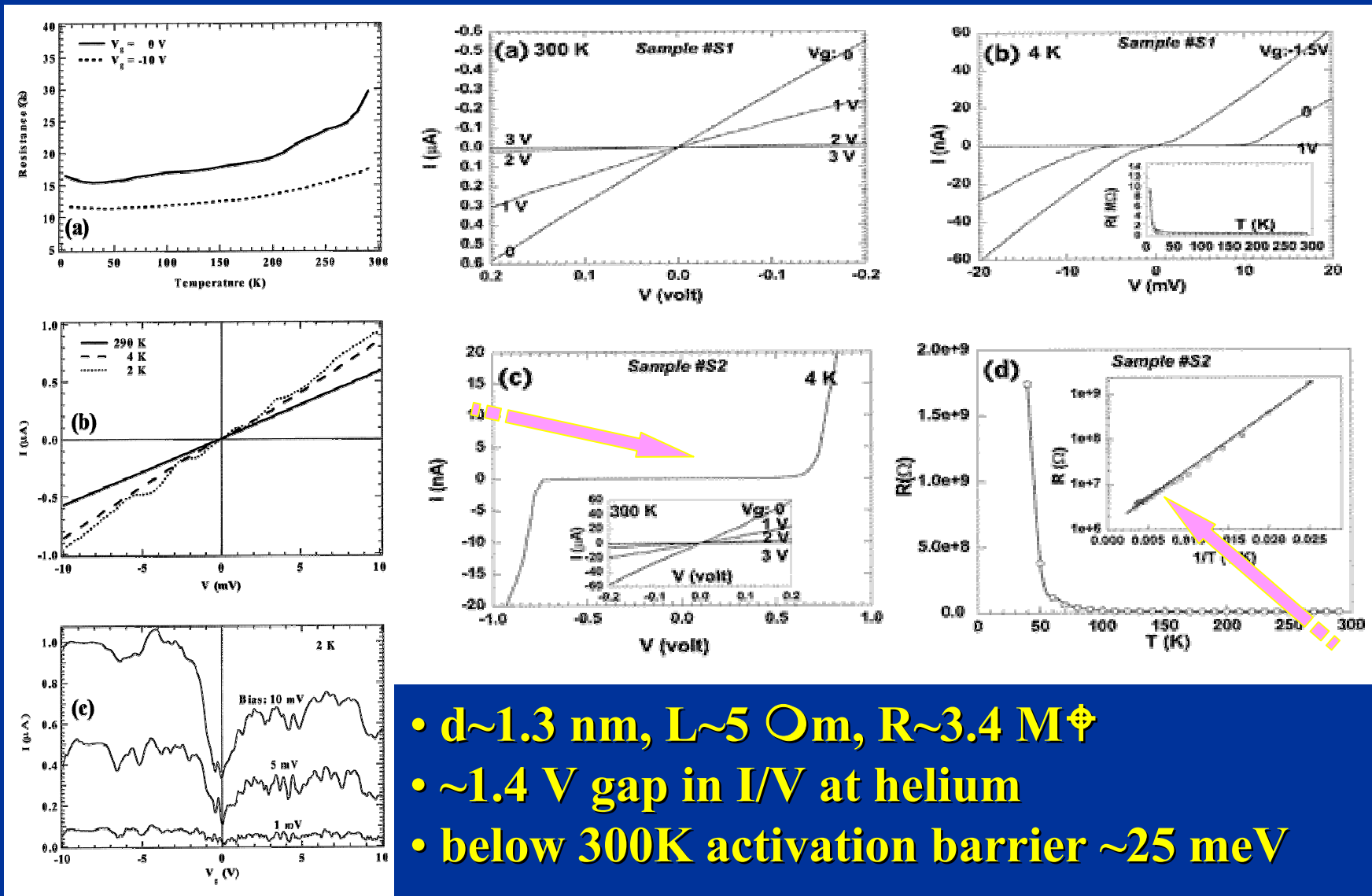
# Me & Se SWNTs



- $d \sim 2.8 \text{ nm}$ ,  $L \sim 3 \text{ } \mu\text{m}$ ,  $R \sim 370 \text{ k}\Omega$
- $\sim 20 \text{ mV}$  gap in I/V at helium
- below 25K activation barrier  $\sim 5 \text{ meV}$



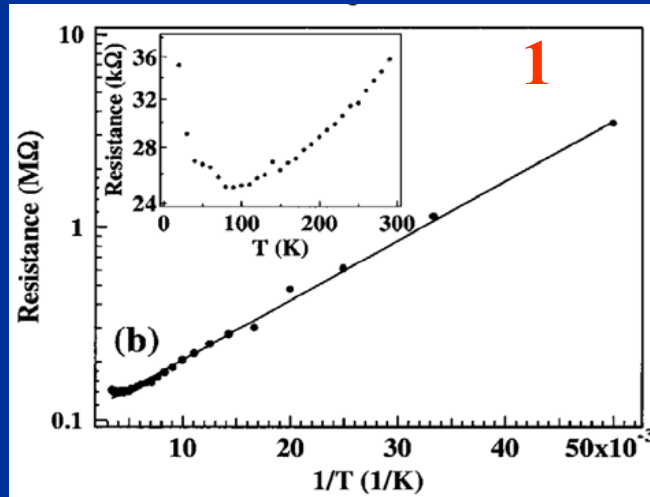
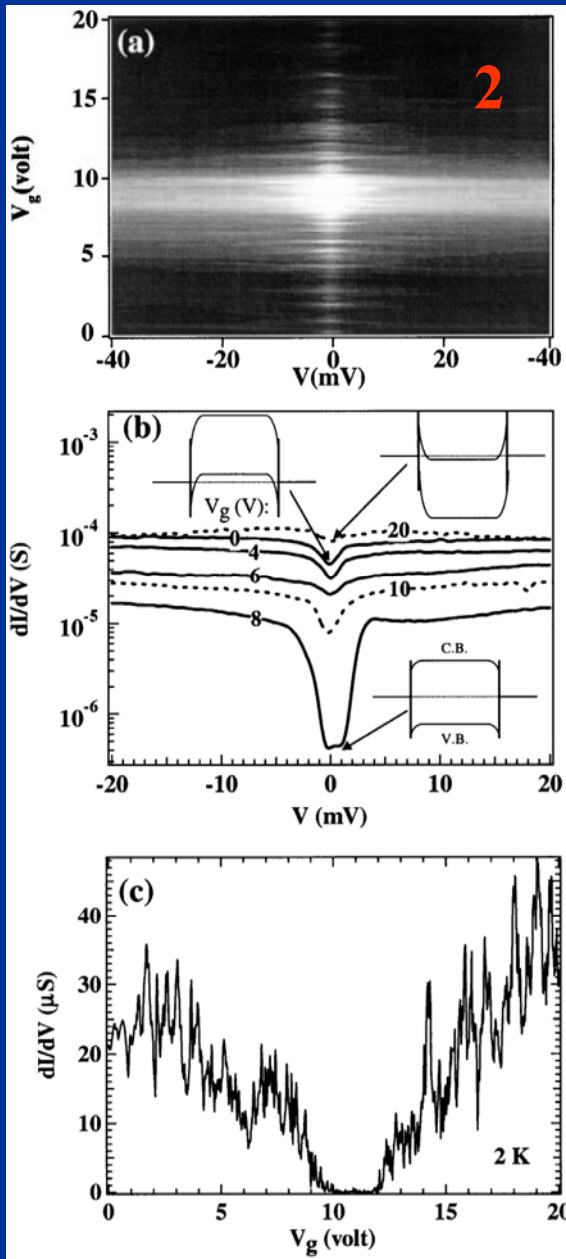
# Me & Se SWNTs



- $d \sim 1.3$  nm,  $L \sim 5$   $\mu$ m,  $R \sim 3.4$  M $\Omega$
- $\sim 1.4$  V gap in I/V at helium
- below 300K activation barrier  $\sim 25$  meV

# Small-gap NT

H.Dai, 1999.



- (a) Grey-scale 2D conductance plot recorded at 2 K. The brightest shade of grey corresponds to the lowest conductance  $\sim 10^{-7}$  S. The darkest shade corresponds to the highest conductance  $\sim 4 \cdot 10^{-5}$  S.
- (b) Conductance at various  $V_g$ . Inset: band diagrams under several gate voltages.
- (c) Zero-bias conductance at  $V_g^*$  vs  $V_g$ .

**Origin of large conductance fluctuations at low bias is unknown.**

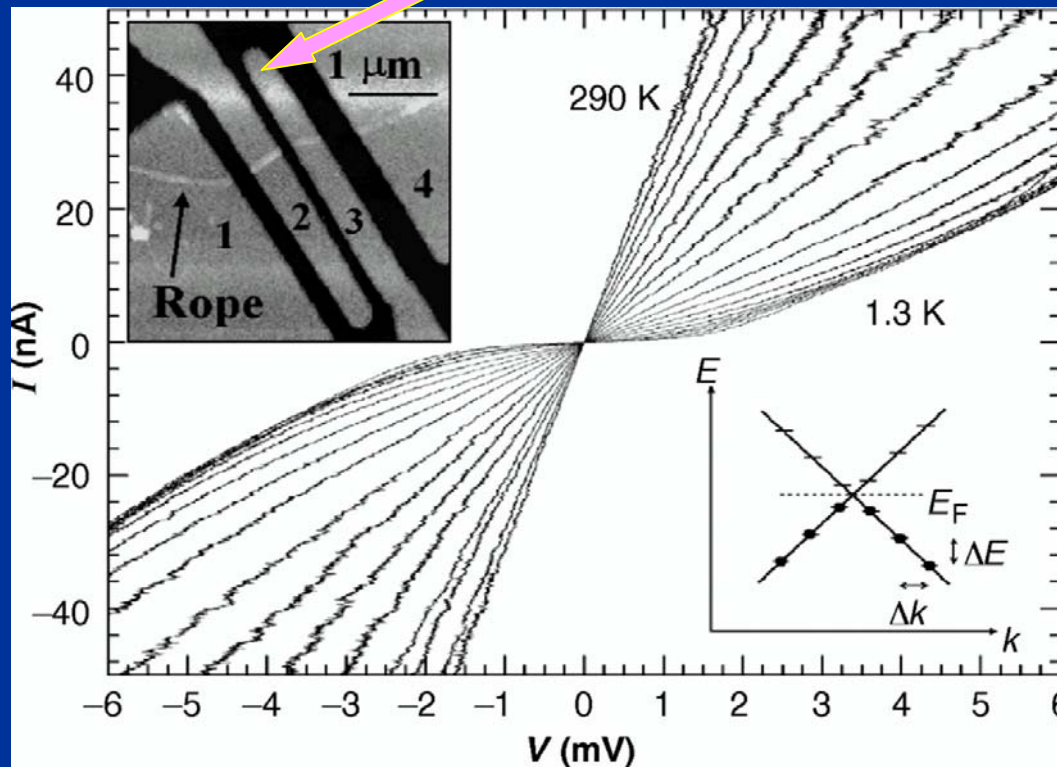
**R vs T gives too small activation energy**

**Linear resistance measured at  $V_g^*$ . Solid line: exp fit with  $E_a \sim 6$  meV. Inset: Resistance at  $V_g = V_g^* - 5$  V and 1 mV bias.**

# SE transport

P. McEuen (1997)

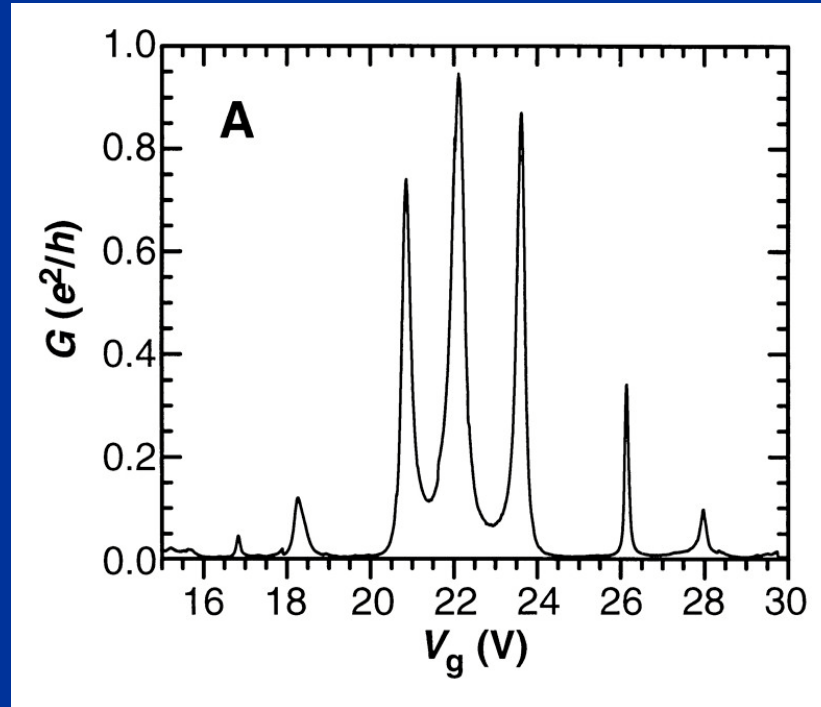
3 nm Cr + 30 nm Au



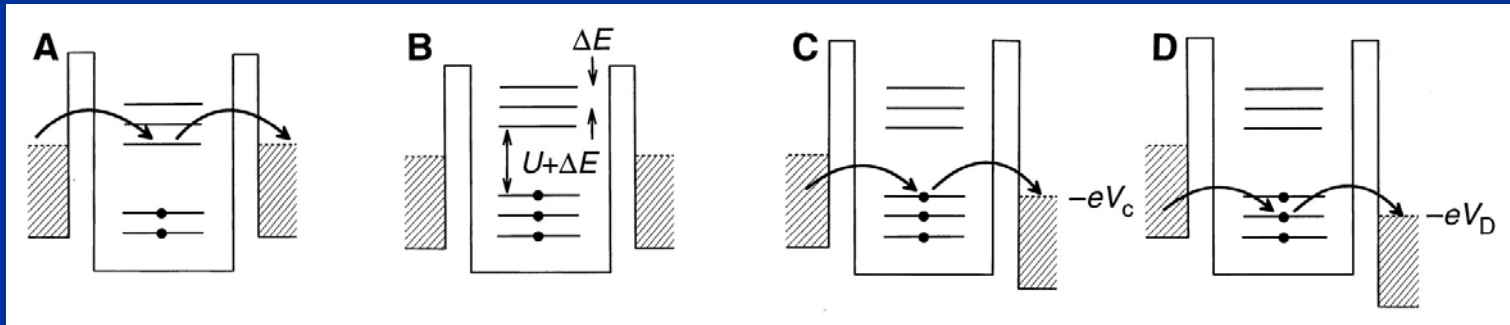
$I$ - $V$  characteristics at a series of different temperatures for the rope segment between contacts 2 and 3. (Left inset) AFM image of a completed device. The bright regions are the lithographically defined metallic contacts, labeled 1 to 4. The rope is clearly visible as a brighter stripe underneath the metallic contacts. Between the contacts (dark region), it is difficult to see the rope because of the image contrast. (Right inset) Schematic energy-level diagram of the two 1D subbands near one of the two Dirac points, with the quantized energy levels indicated. Here  $k$  points along the tube axis.

# SE transport

P. McEuen (1997)

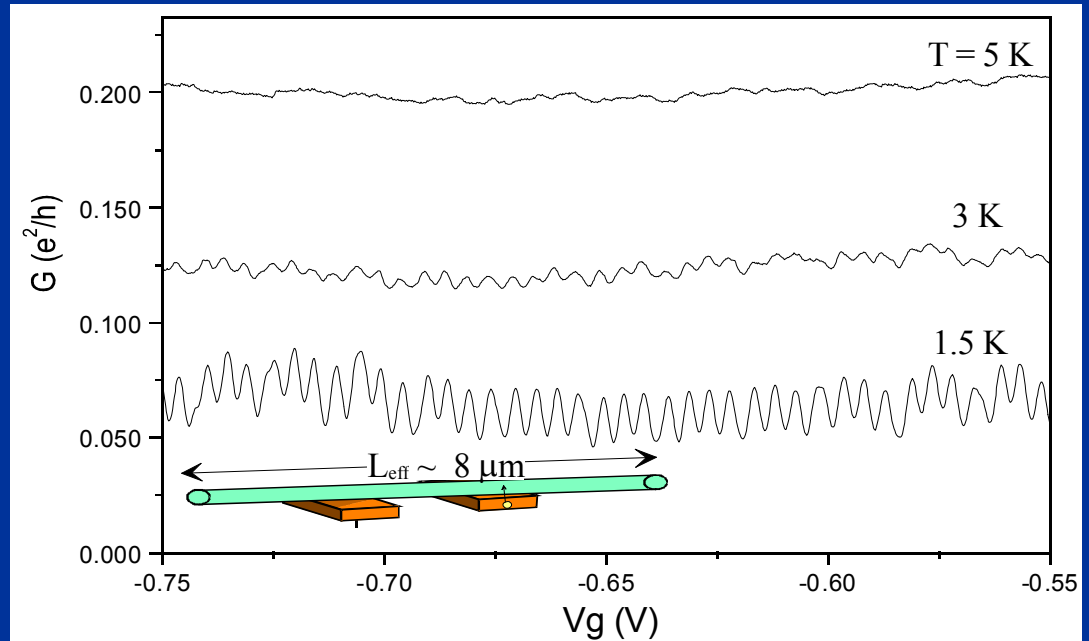
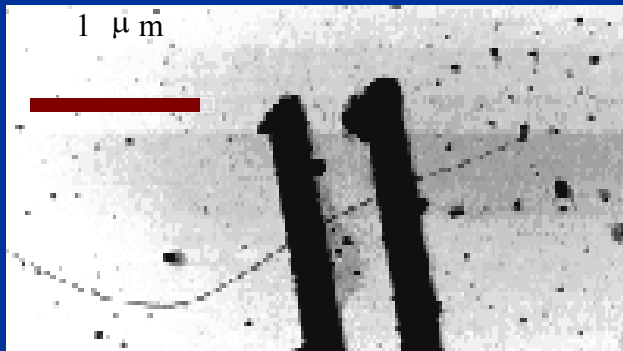


Conductance  $G$  versus gate voltage  $V_g$  at  $T = 1.3$  K for the rope segment between contacts 2 and 3.



# CB oscillations

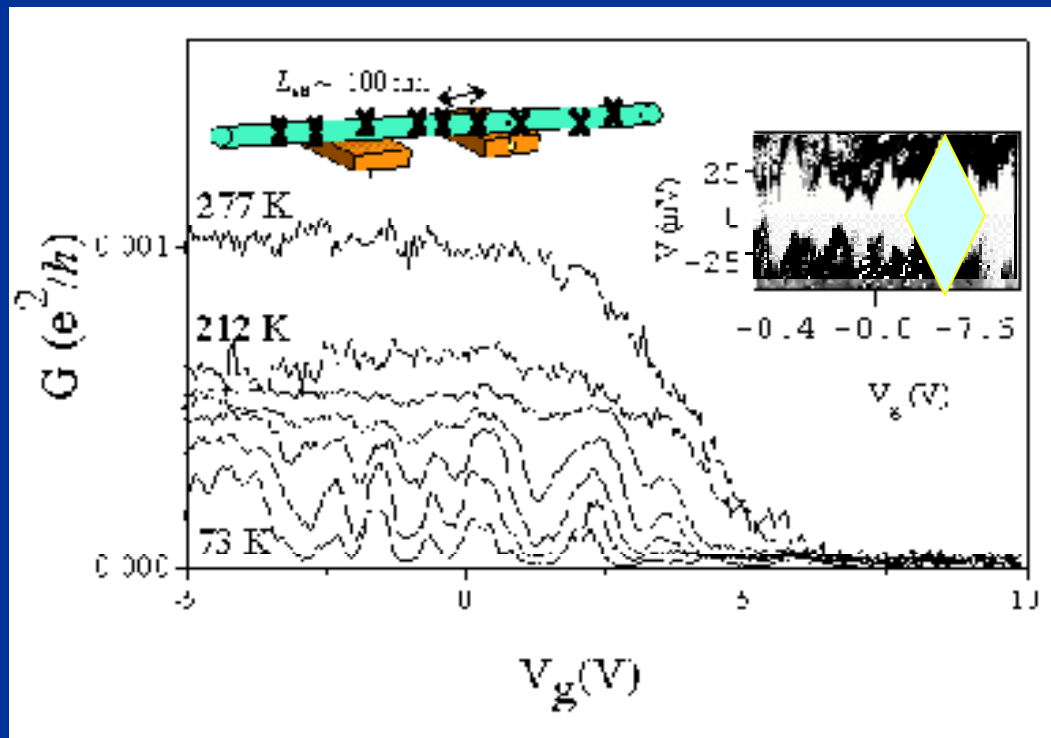
P. McEuen (1999)



**Me-SWNT with “bad” tunnel contacts shows Coulomb Blockade and (at low temperature  $\sim k_B E_C \sim 0.5 \text{ meV}$ ) periodic oscillations corresponding to  $L_{\text{eff}} \sim \langle \text{size of NT} \rangle$ .**



# Se-SWNT as a series of QDs



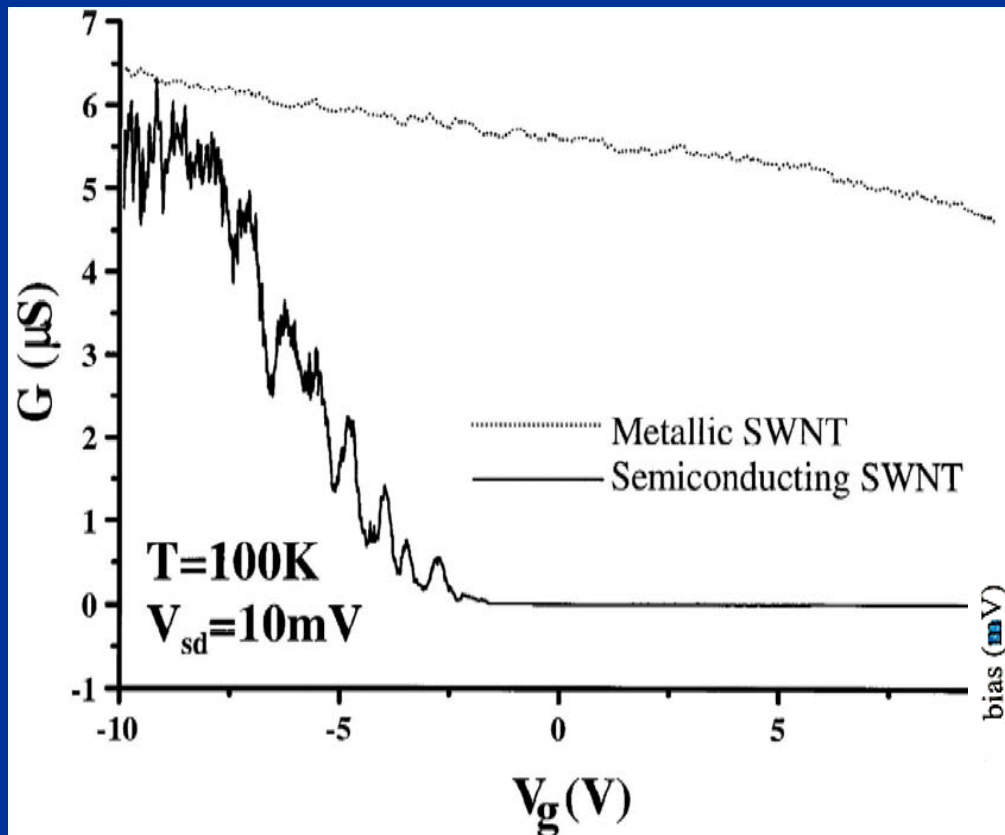
P. McEuen (1999)

$$C \sim L$$

$$E_c \sim e^2/C \sim e^2/L$$

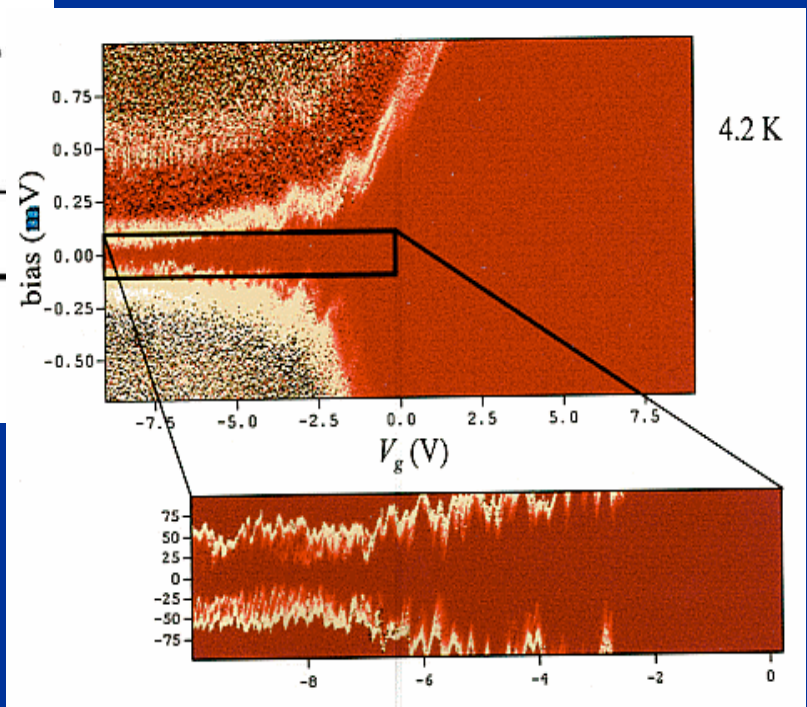
In the same geometry Se-SWNT (tunnel contact) shows at low temperature  $\sim 25\text{meV}$ ) aperiodic oscillations. These could be related to CB in the series of QDs.

# Se SWNT conductivity



P. McEuen (2000)

Se-SWNT conductivity oscillations at low bias (and low  $T$ ) can be attributed to tunneling in multiple QD...

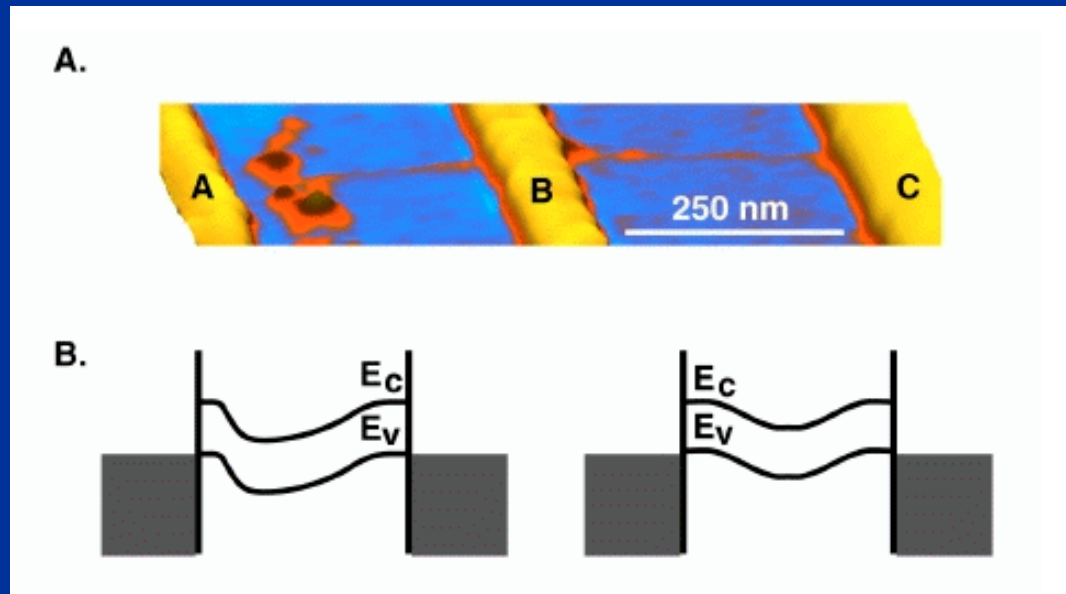
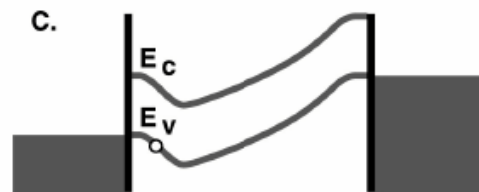
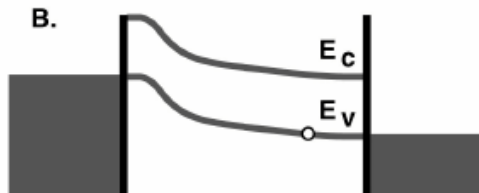
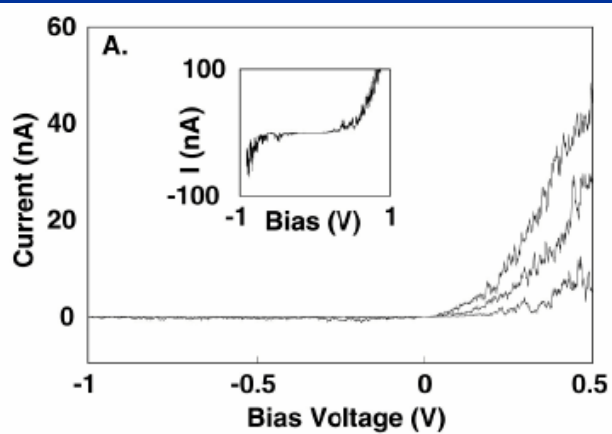


...or, alternatively, to 1D van-Hove singularities probed by gate voltage

# Subband population

A. T. Johnson Phys Rev Lett 1999

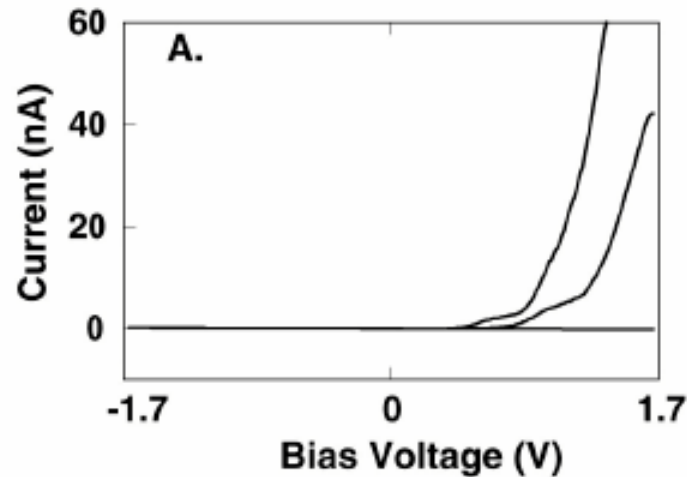
- Experiment which can indicate subsequent population of 1D-subbands



Studied structure (two parts, one is contaminated)

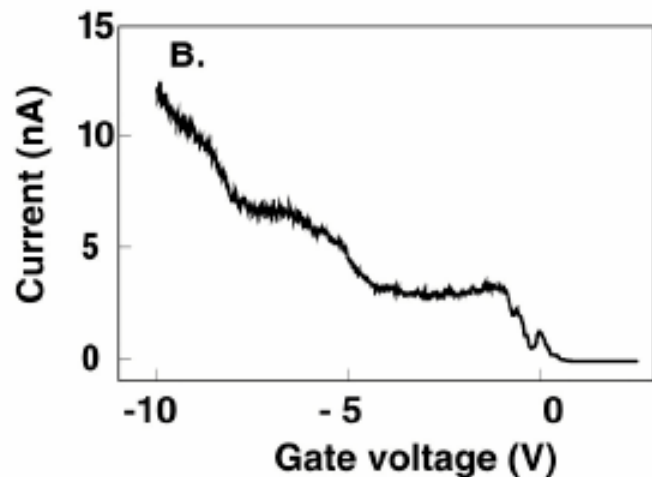
# Subband population

A. T. Johnson Phys Rev Lett 1999



(A) I-V curves for the nanotube diode at 77 K and  $V_g = 25, 0, 15$  V (top to bottom). Stepwise current increases with bias are due to sharp van Hove singularities in the density of states at the edge of 1D electronic subbands.

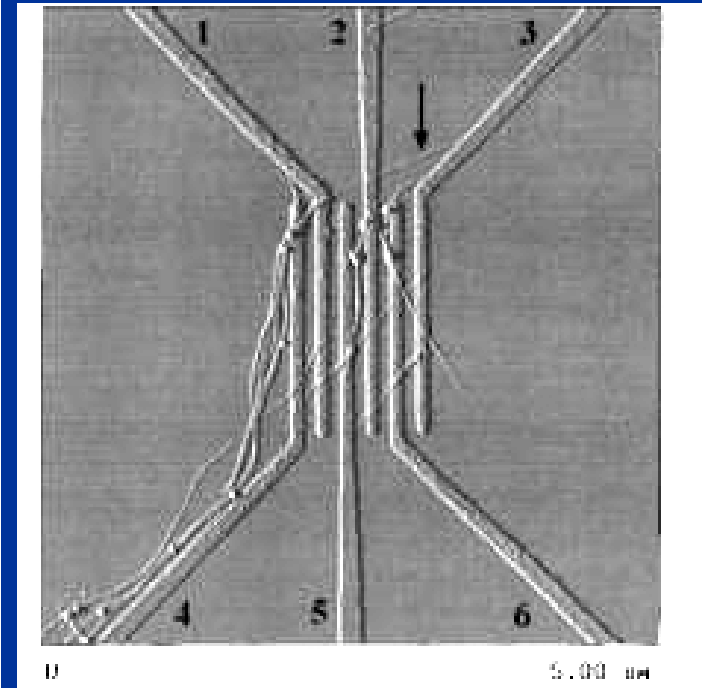
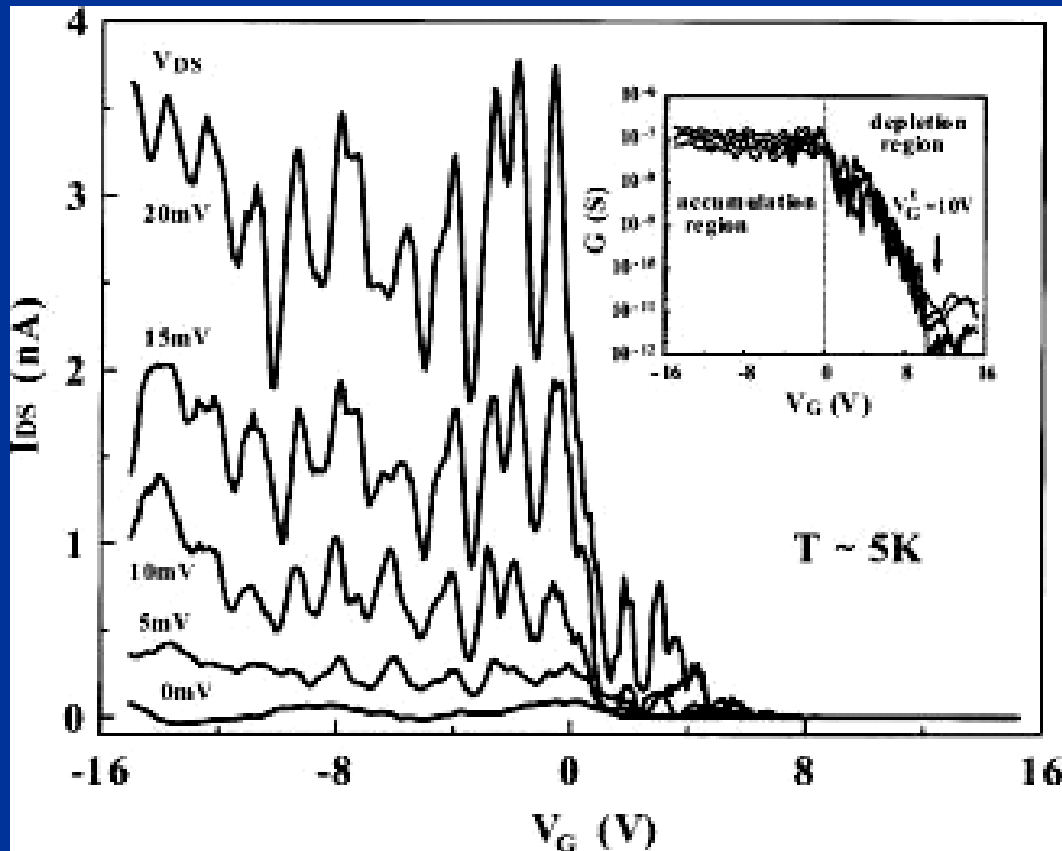
(B) Current vs gate voltage in the nanotube at 1 V forward bias. Steps occur when another 1D subband transports charge through the diode.



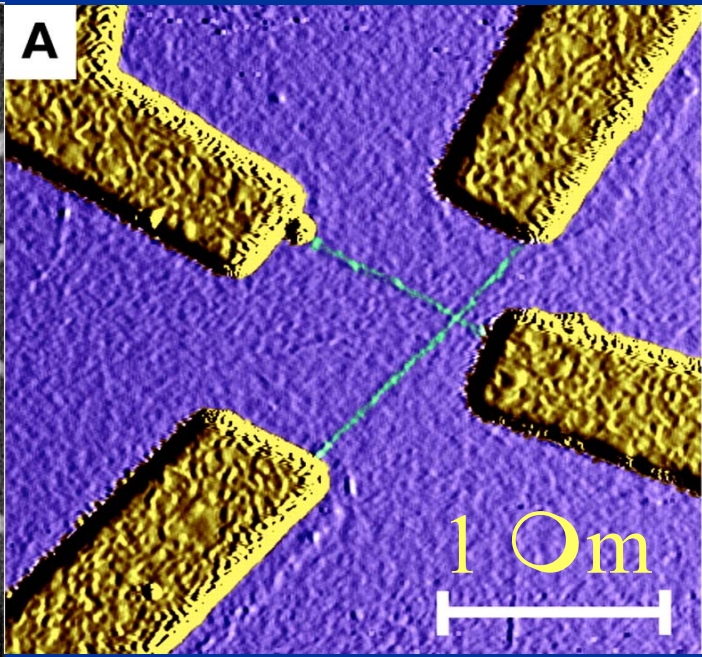
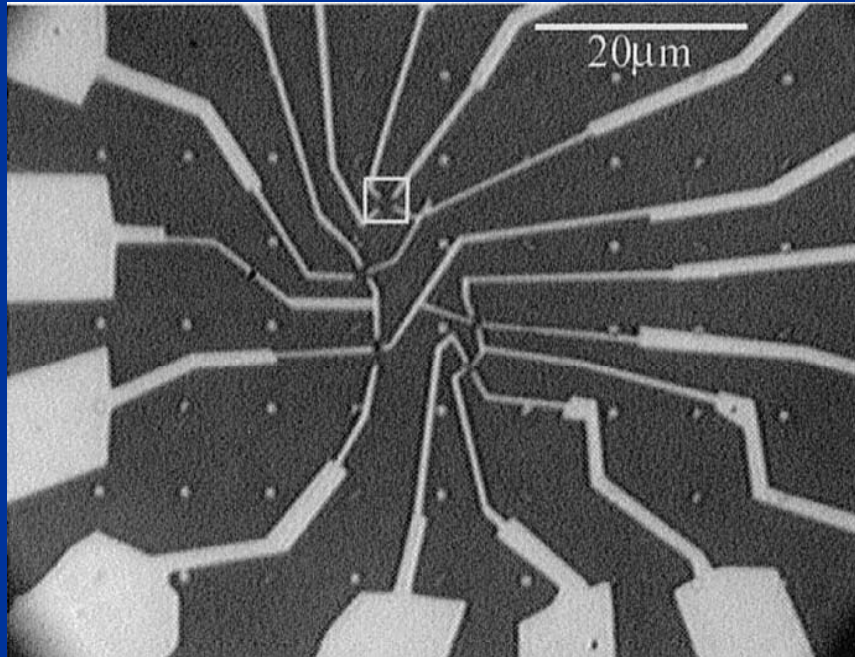
# Subband population

S.Roth Applied Physics Letters, 1999

- Room temperature (not shown) excludes CB-oscillation
- energy separation between peaks too small to come from one SWNT



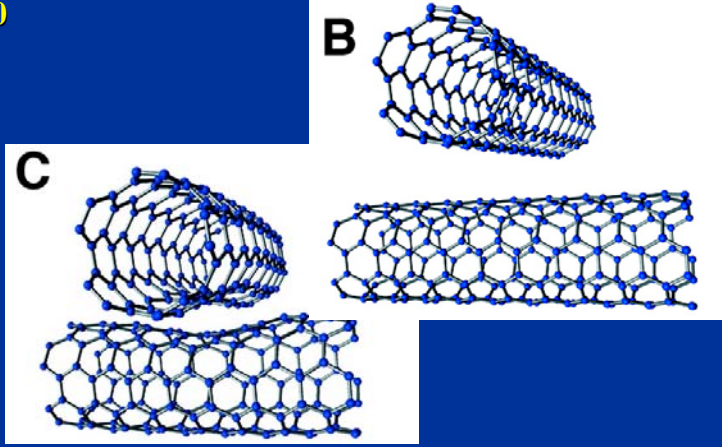
# NT Junctions



P.McEuen et.al., Physica E (2000)

P.McEuen et.al. Science 2000

- vdW attraction to substrate can result in NT deformation
- local perturbation of 1D-structure
- larger NTe-NTe interaction

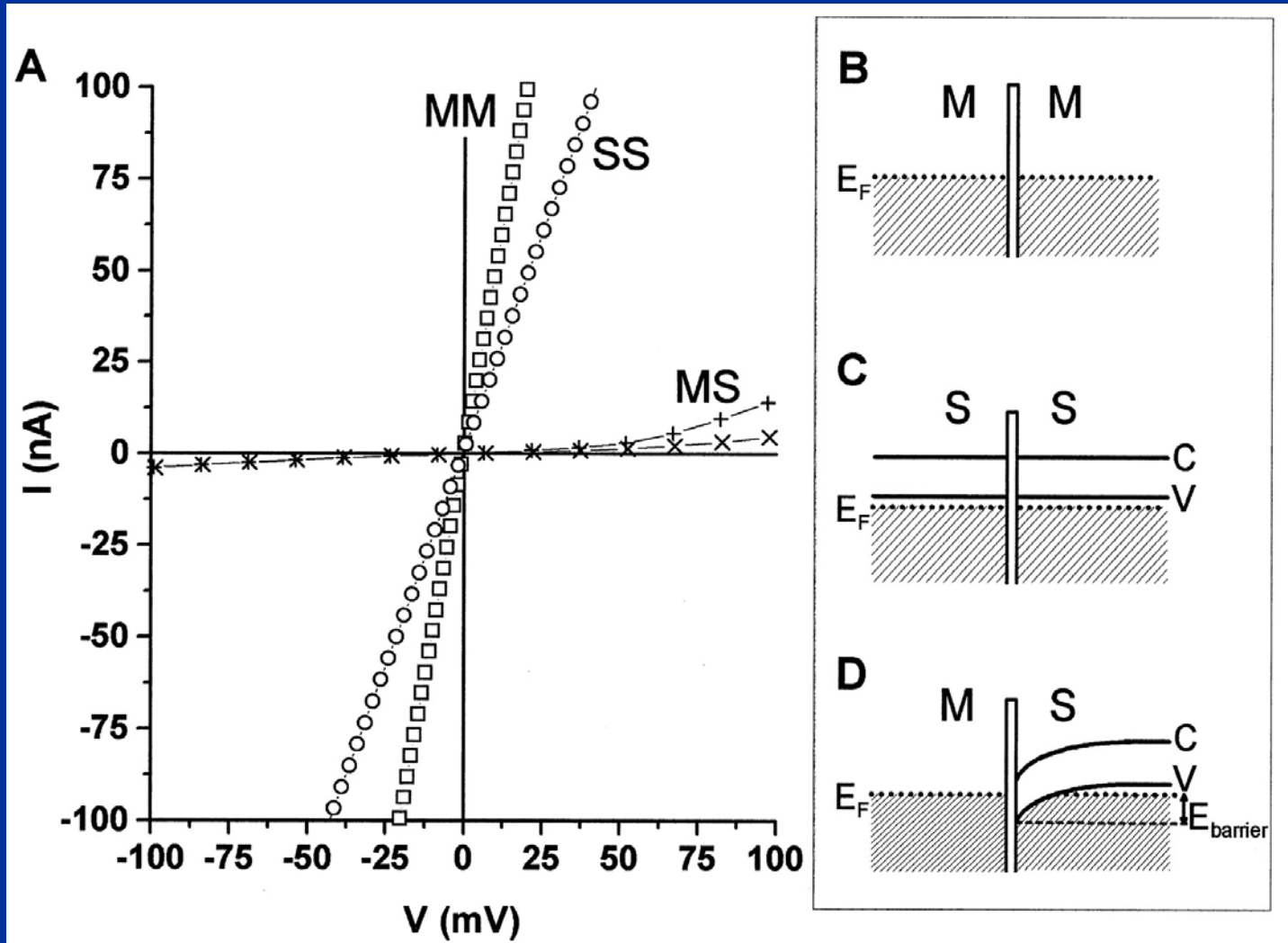


# Me-Me, Se-Se & Me-Se NTJn

•SB model invoked to explain difference in I/Vs

MM  $\sim 200 \text{ k}\Omega$

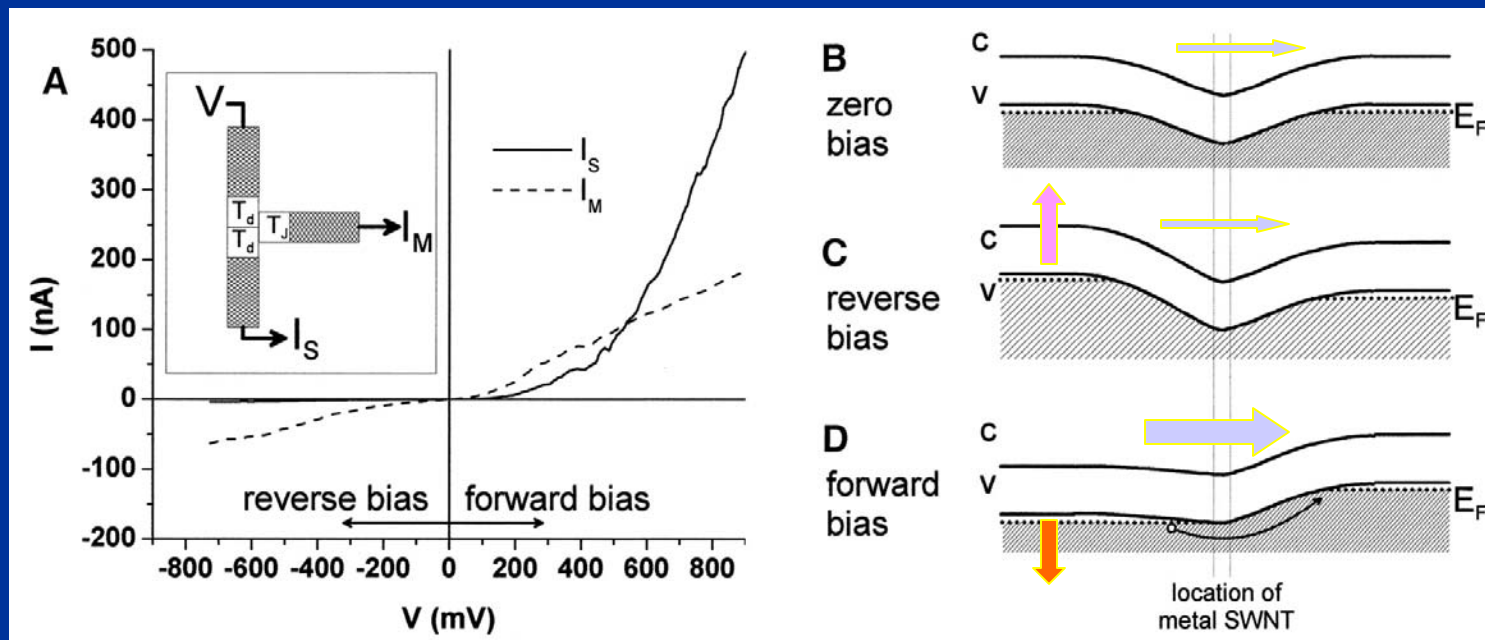
SS  $\sim 3 \text{ M}\Omega$



P.McEuen et.al. 2000

# Me-Se NTJn

P.McEuen et.al. 2000

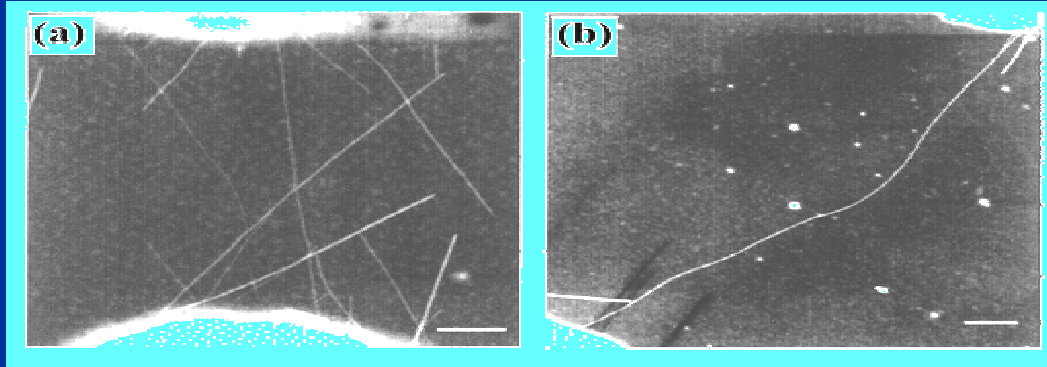


**Rectifying behavior of 2-SB NT-Jn device**

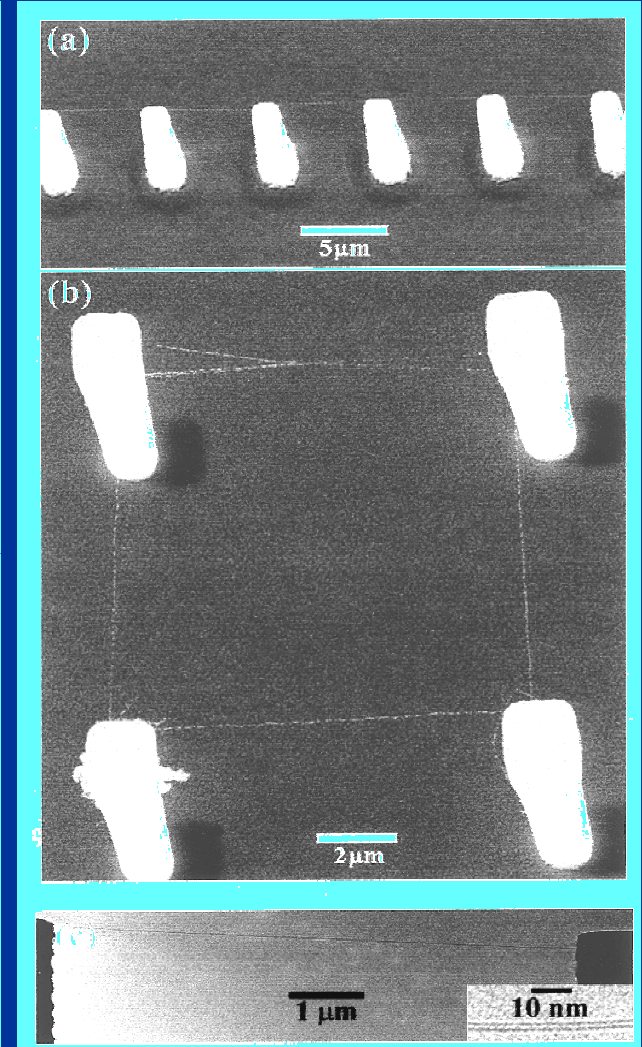
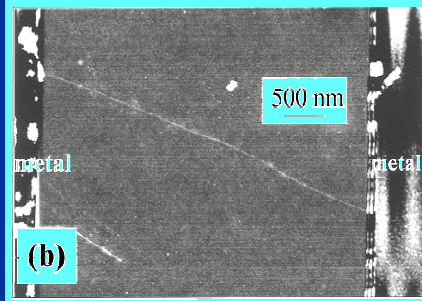
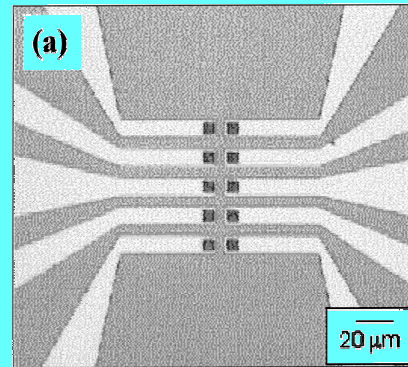


# Fabrication technique

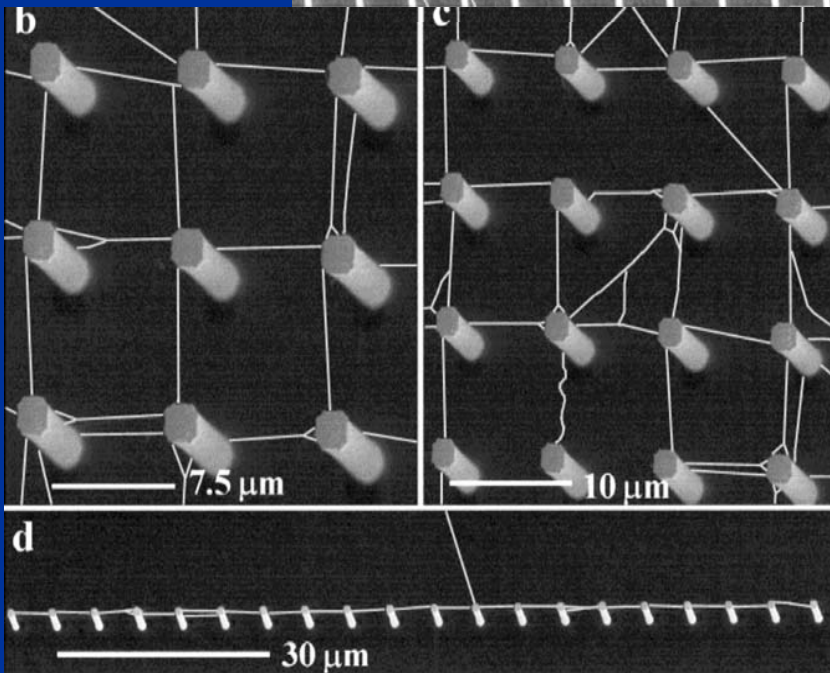
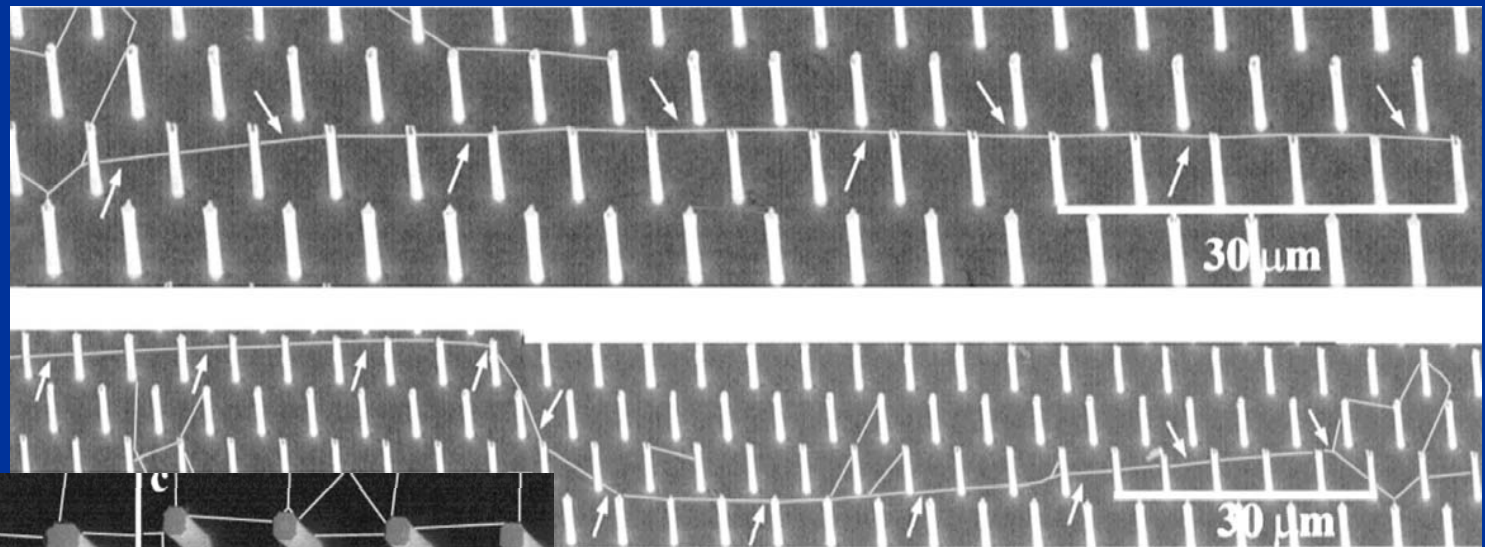
H.Dai, J. Phys. Chem. B., 1999.



- CVD is advanced method to make NT device/circuit
  - desired geometry
  - better contact
  - suspended tubes
  - “controlled” size/d



# NT “Power Line”



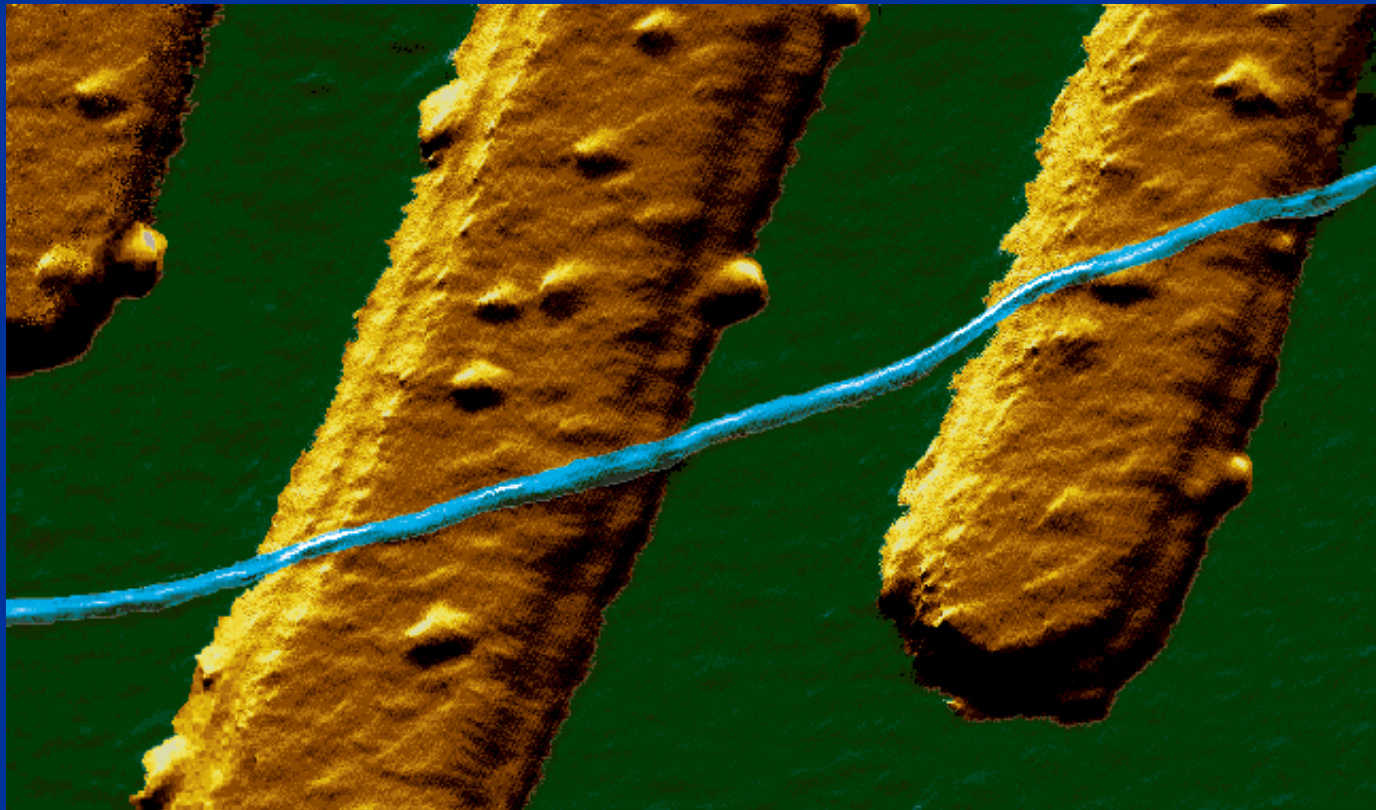
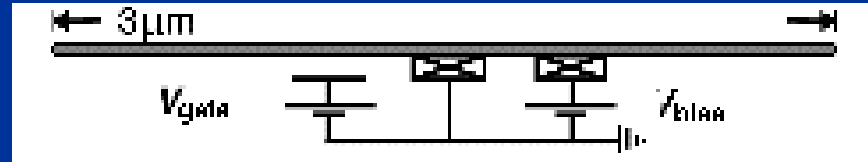
H.Dai et.al., Adv. Mater. 2000

**CVD allows connected lines of NTs between Si pillars as long as 150  $\mu\text{m}$ . Multiple connections appear.**

# SWNT FET: TUBEFET

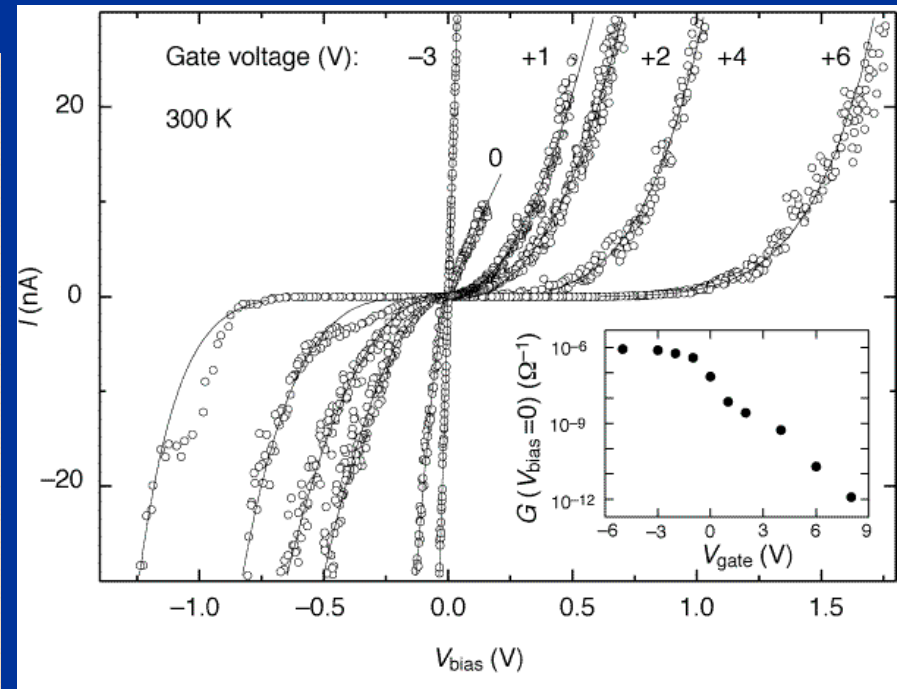
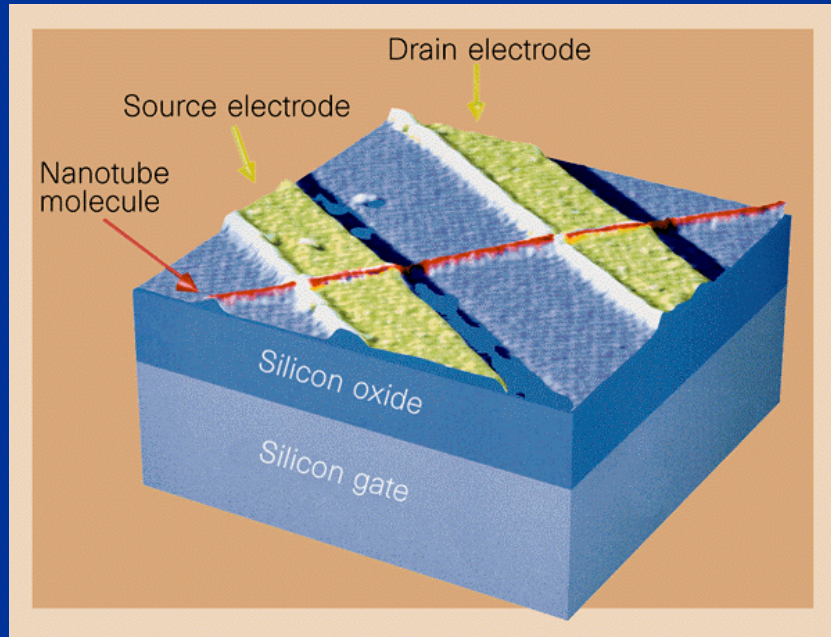
S.J.Tans et.al., Nature (1997)

- Au electrodes
- spin-coating of SWNTs



# SWNT FET: TUBEFET

Tans et.al. and (1998)



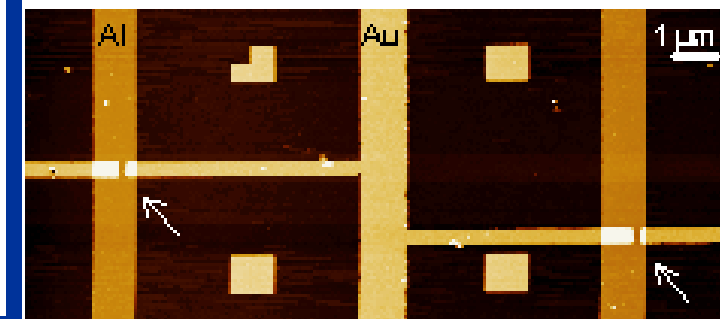
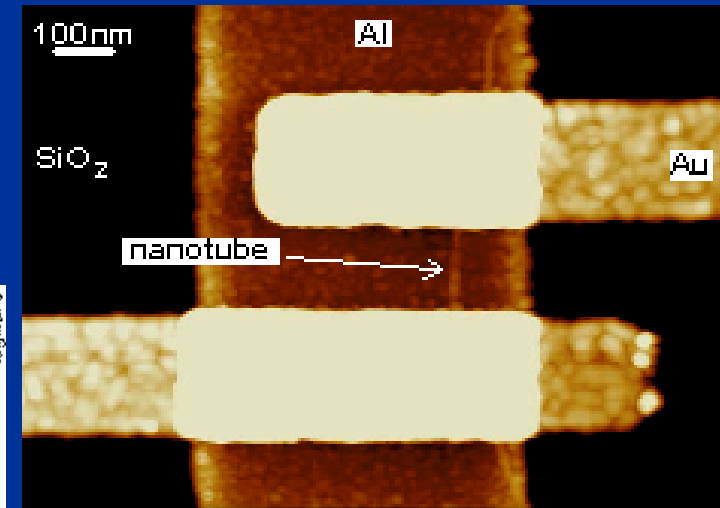
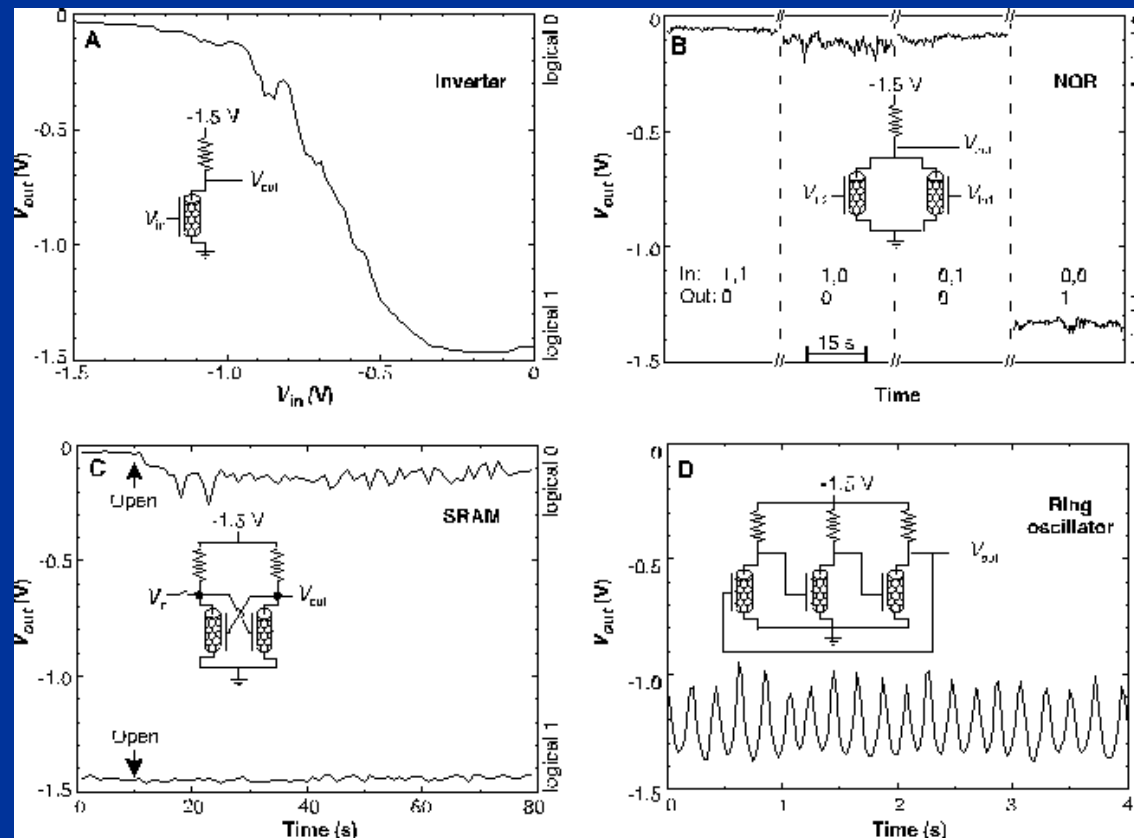
Two probe  $I-V_{\text{bias}}$  curves for various values of the gate voltage ( $V_{\text{gate}}$ ). Data were taken at room temperature and in vacuum ( $10^{-4}$  mbar). A negative  $V_{\text{gate}}$  leads to ohmic behaviour while a positive  $V_{\text{gate}}$  results in a strong suppression of the current at low bias voltage and nonlinear  $I-V_{\text{bias}}$  curves at higher bias. Inset, conductance at  $V_{\text{bias}} = 0$  as a function of  $V_{\text{gate}}$ .

- Hole conductivity correlates with STS data: band-bending model
- High contact resistance  $R_{\text{total}} \sim G^{-1}$

# Toward NT Electronics

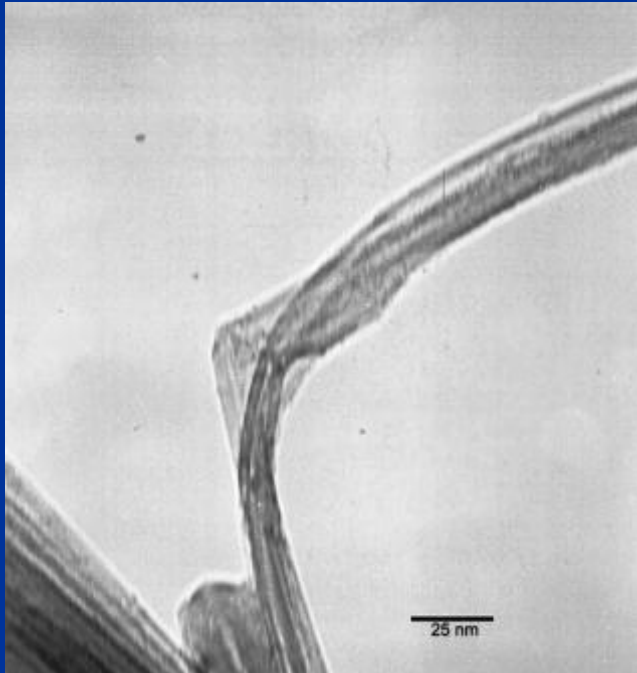
A. Bachtold et al., Science (2001)

## Logic circuits with NT transistors



# Defects for NT-Electronics

P. M. Ajayan et.al., APL, 2000



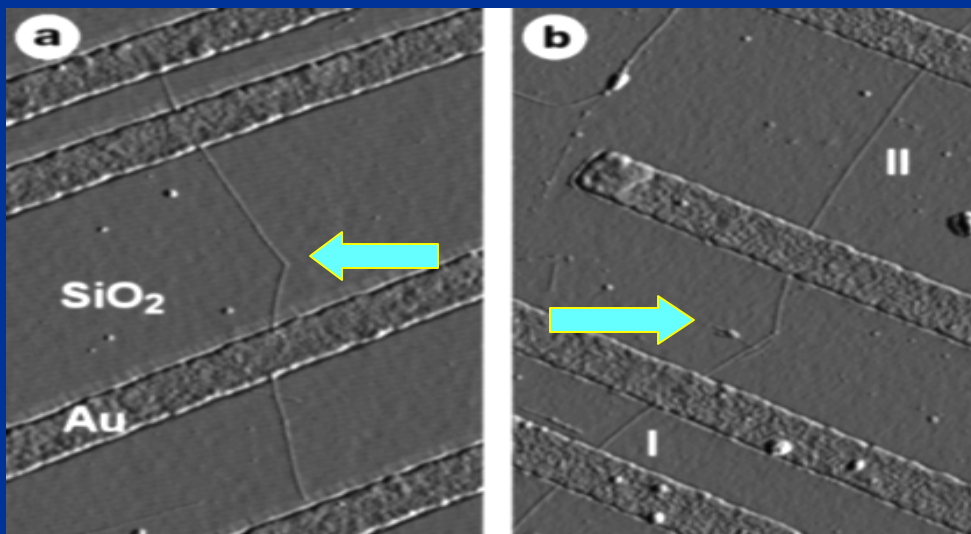
**Kink appear if NT is elastically or plastically deformed or contains 5/7 defect**

**Defect scatters carriers and divides two regions of different symmetry (5/7 pair is a node of linear disclination in graphene lattice)**

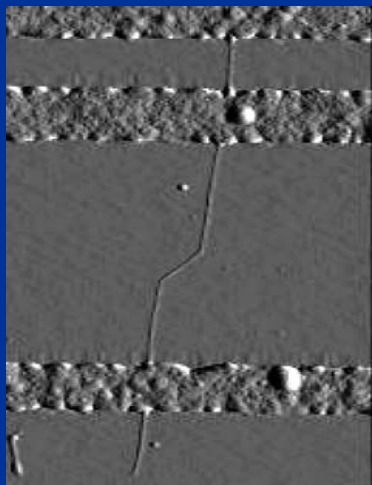
V.H.Crespi et.al., PR,L 1996



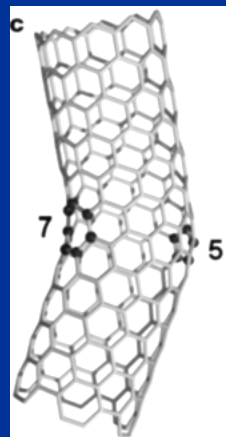
# Defects for NT-Electronics



Nanotubes that contain a single kink of  $36^\circ$  and  $41^\circ$



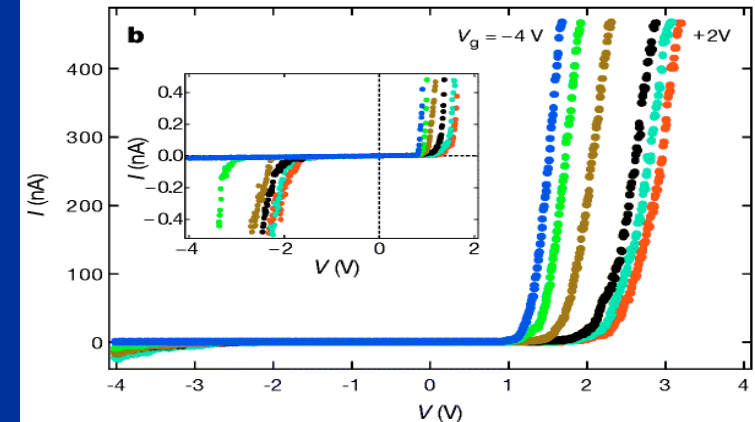
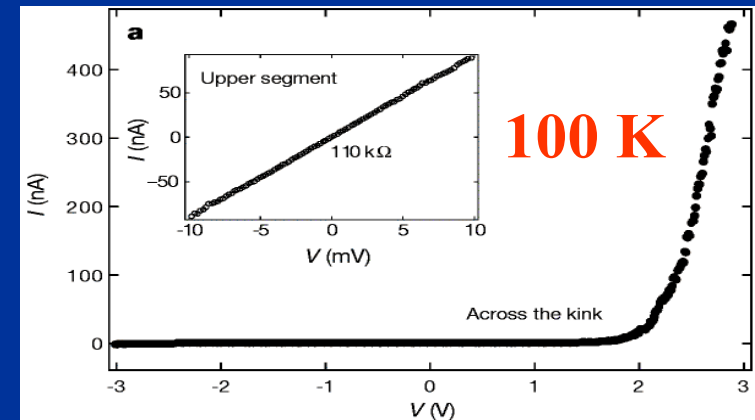
double-kink



5-7 model

$V_G \sim -4, -2, -1, 0, 1$  and  $2$  V

Dekker (1999)  
NT kink - Me-Se SWNT-Jn



Current-voltage characteristics across the Me-Se SWNT junction show rectifying behavior.

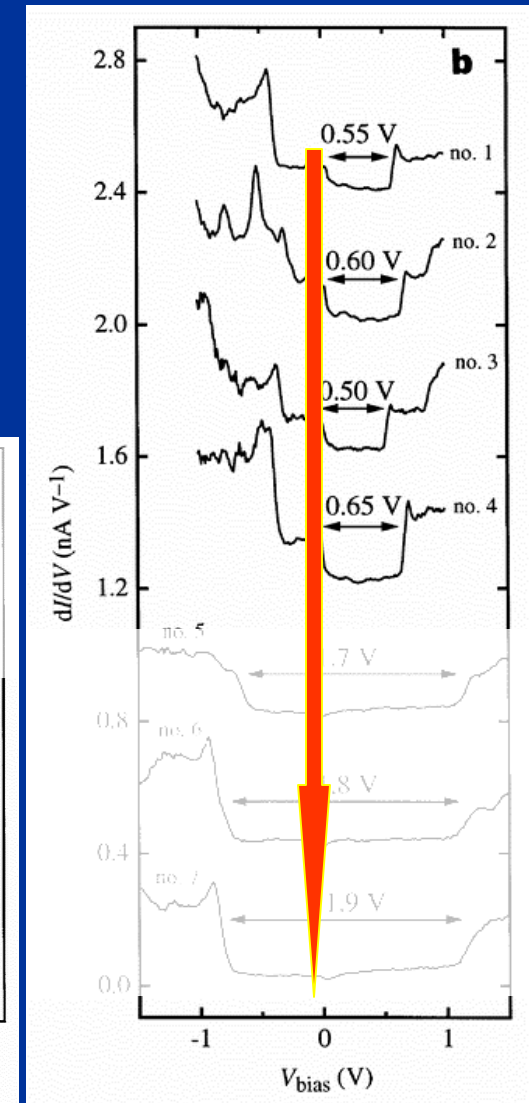
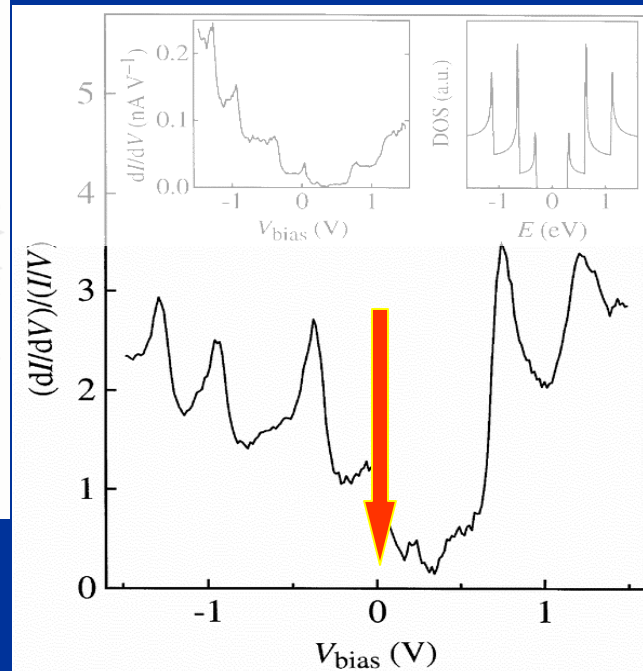
# Me and Se SWNT: STS

Graphite sheet scrolling • 2 types of STS

Dekker (1999)



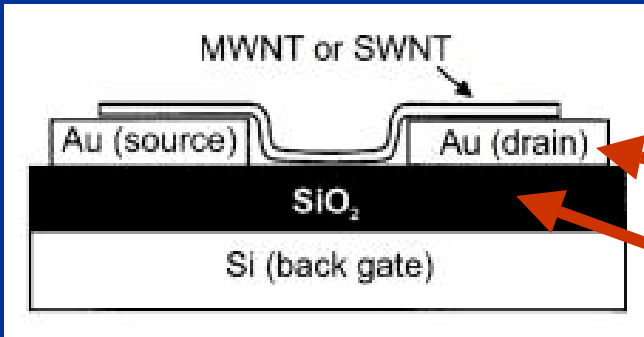
- gap
- pinning of  $E_F$  in Se-SWNT to  $E_V$
- zero-bias dip
- STS reflects DOS





# Field Effect Transistors

Ph.Avouris 1998

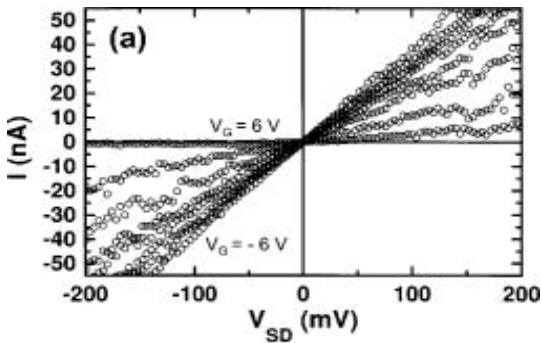


• Schematic cross section of FET device.

140 nm  
30 nm

$R_c \sim 1.1 \text{ M}\Omega$

$R_{\text{total}} = 2.9 \text{ M}\Omega$



Output and transfer characteristics:

(a)

I

—

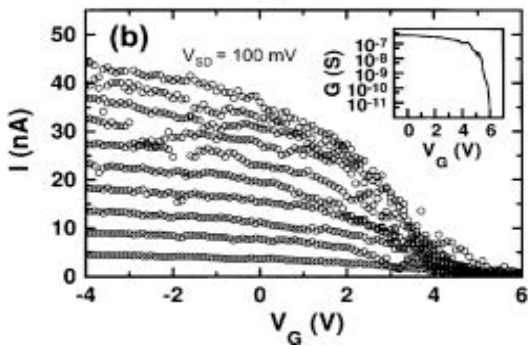
$V_{SD}$  curves measured for  $V_G =$

—

6, 0, 1, 2, 3, 4, 5, and 6 V.

(b)

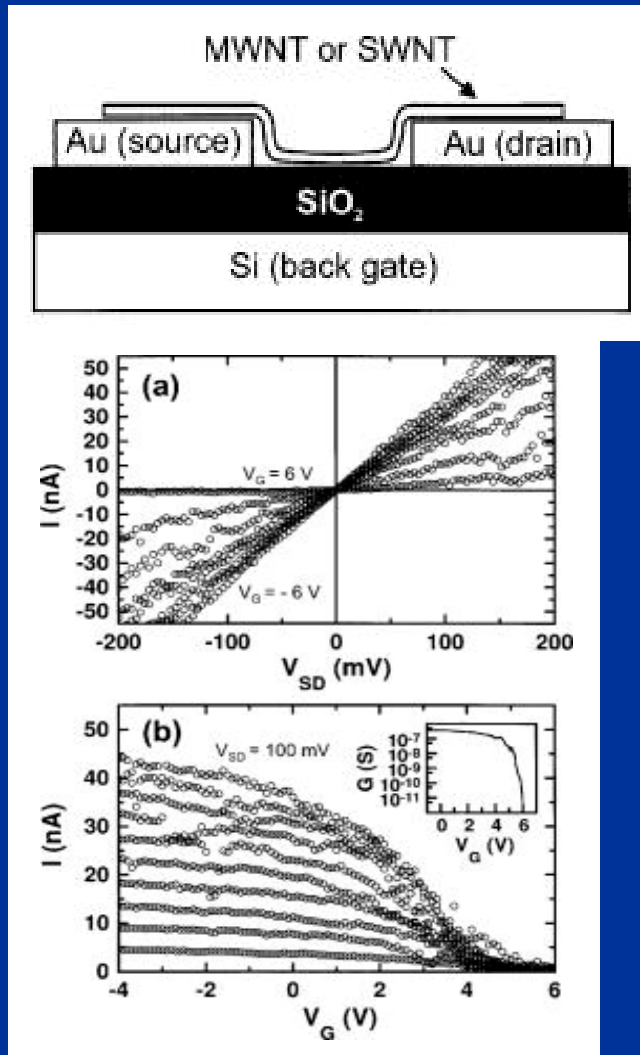
I



—

# Field Effect Transistors

Ph.Avouris 1998



- Inherent homogeneous doping of SWNT-FET
- diffusive transport

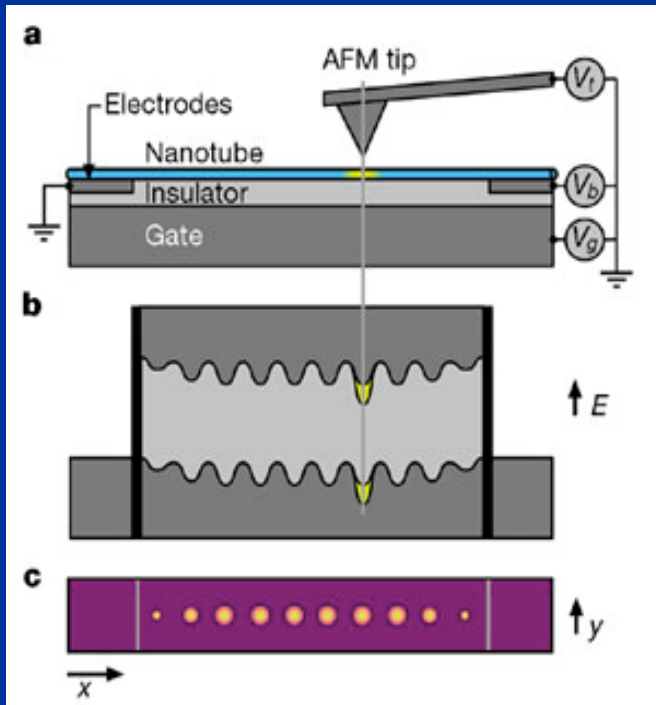
“If the band-bending [results in doping], a positive gate voltage would generate an energy barrier of an appreciable fraction of  $eV_G$  in the center of the tube (gate/NT distance is shorter than the source/drain separation). Threshold voltage to deplete the tube center would be determined by the thermal energy available for overcoming this barrier. Thus, it should be much lower than the 6 V observed”.

# SGPI technique

scanning-gate potential-imaging  
technique

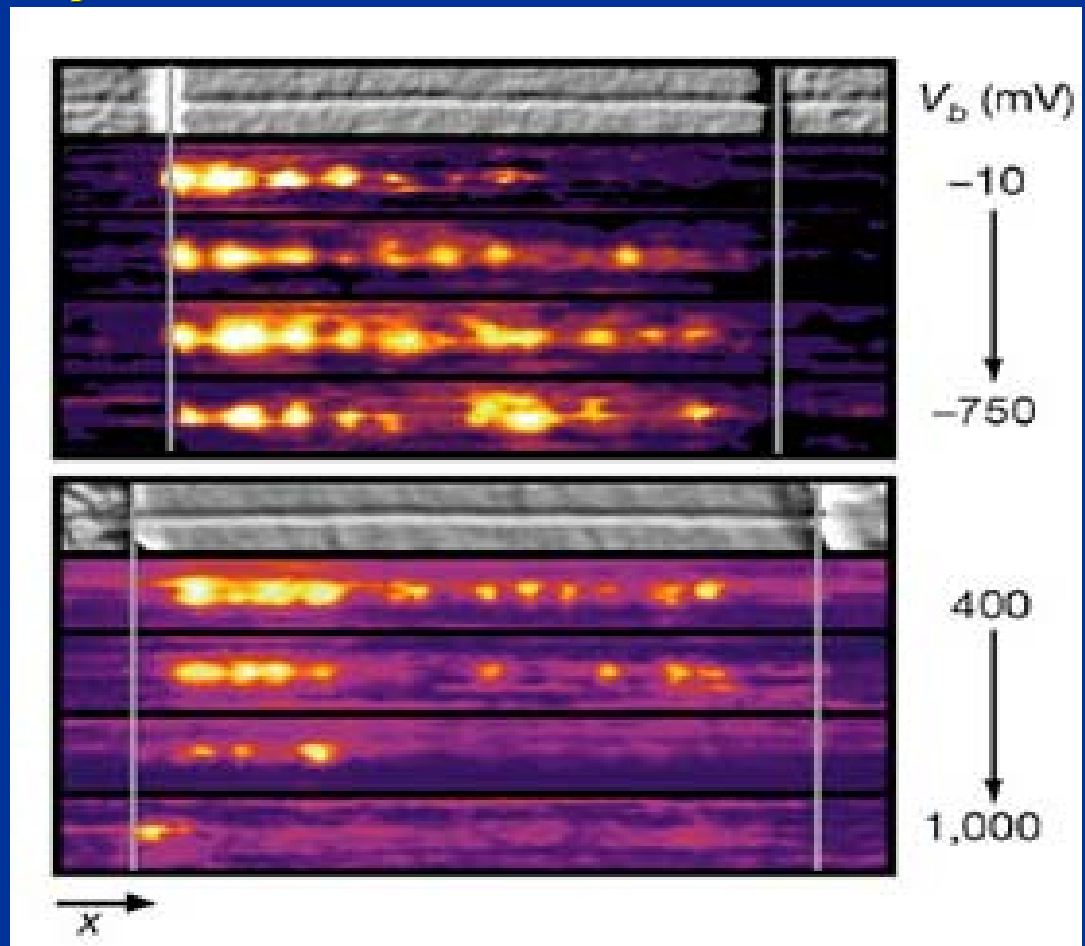
Dekker (2000)

$V_{tip} \sim 0.5V$  (10nm above surface)  $V_G \sim -6V$



#1 Pt (25 nm);  $L_{channel} \sim 650$  nm

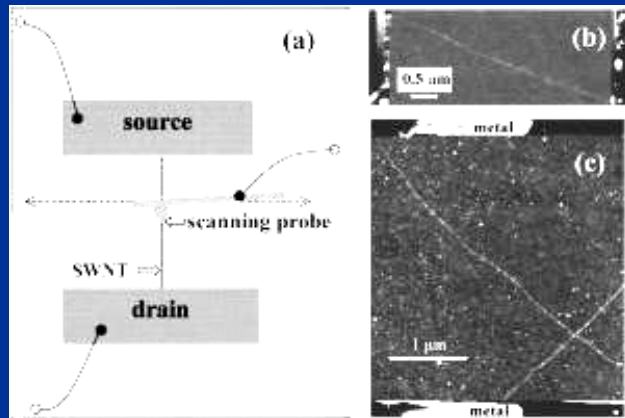
#2 Au (embedded);  $L_{channel} \sim 750$  nm



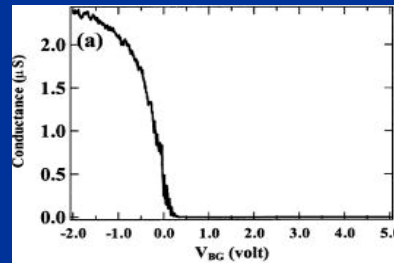
# Local gating with AFM

H.Dai 2000

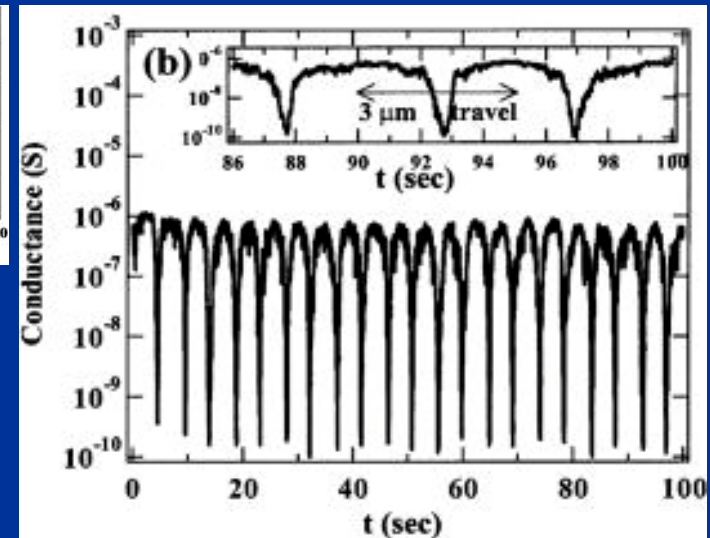
## Gating individual SWNT



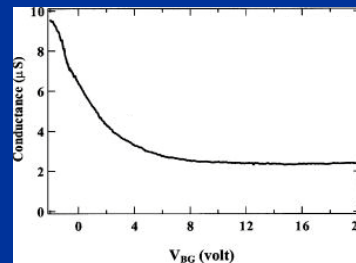
- (a) Scheme of setup
- (b) AFM image of SWNT device.
- (c) AFM image of a SWNT cross.



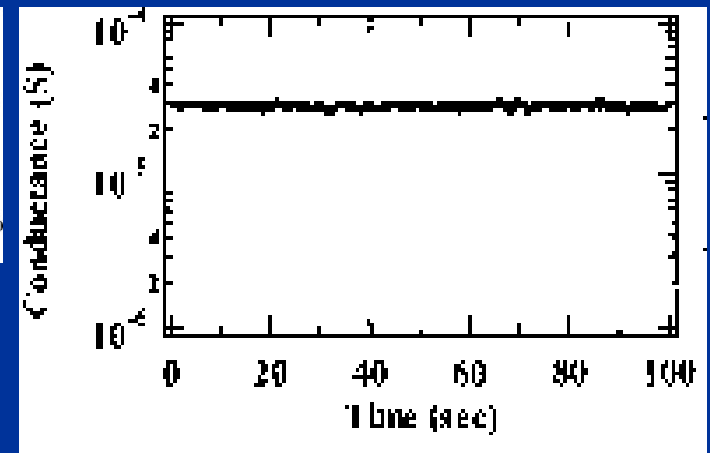
Conductance vs  $V_G$  for Se-SWNT.



Conductance vs time under AFM gating for Se-SWNT. Inset: zoomed-in data between  $t = 86-100$  s.



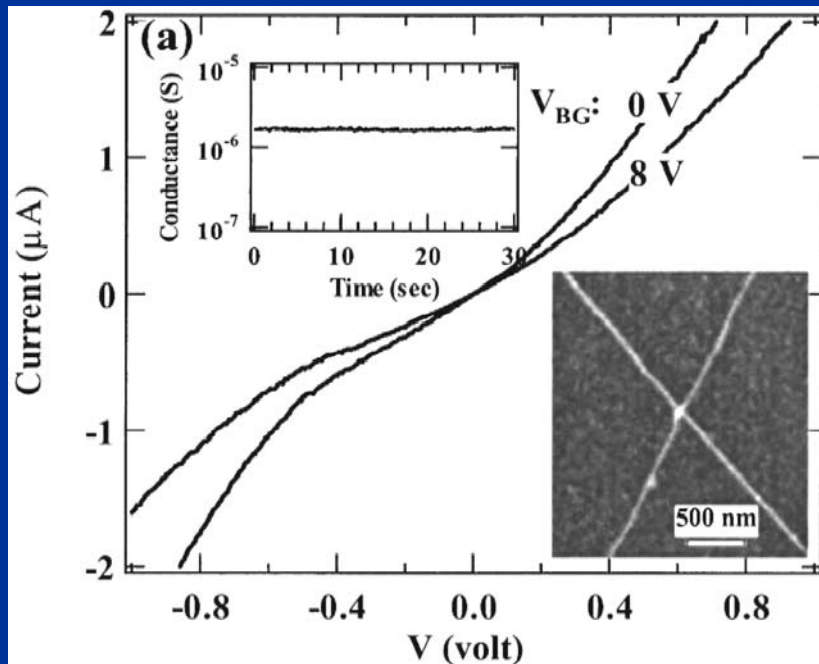
Conductance vs  $V_G$  for Me-SWNT.



Conductance vs time under AFM gating for Me-SWNT

# Local gating with AFM

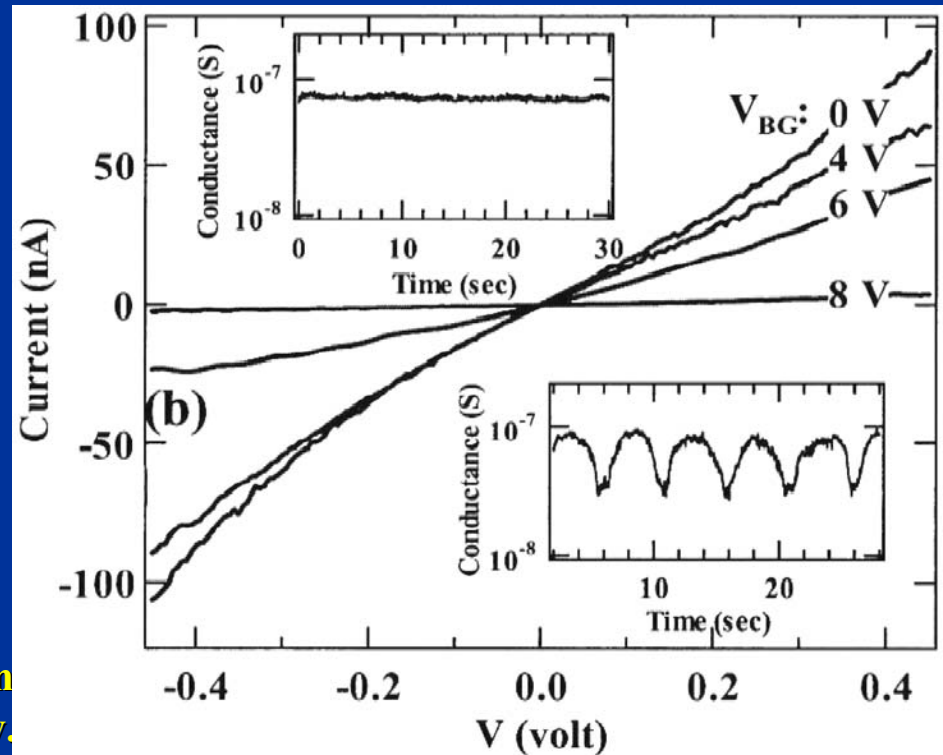
H.Dai 2000



I-V characteristics of a metal-semiconductor SWNT junction. Right and left insets: AFM gating results on the Me-SWNT and Se-SWNT, respectively.

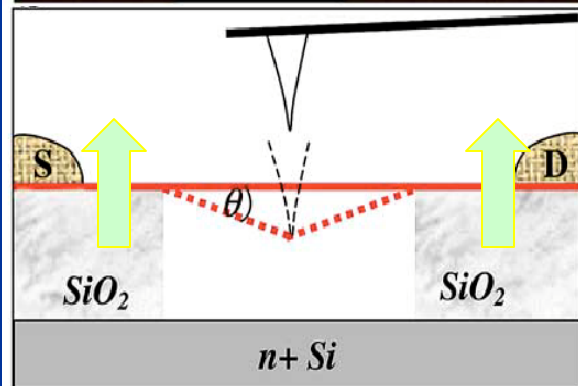
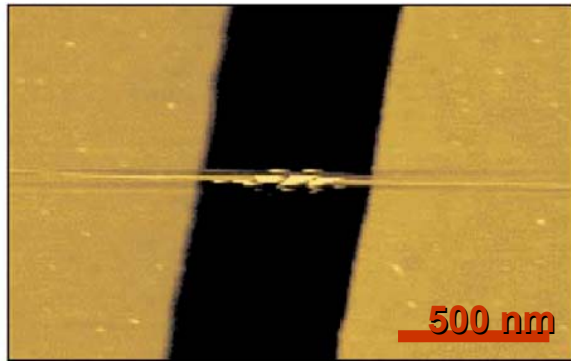
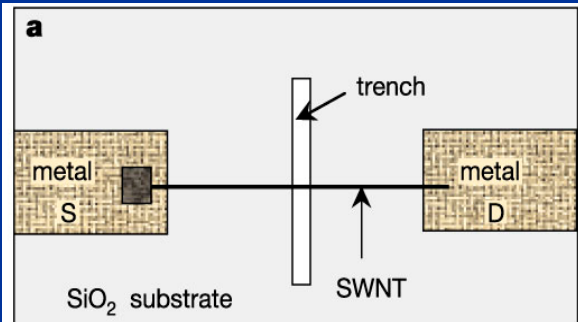
## Gating nanotube junctions

I-V of a metal-metal SWNT junction. Left inset: AFM gating. Right inset: AFM image of the junction



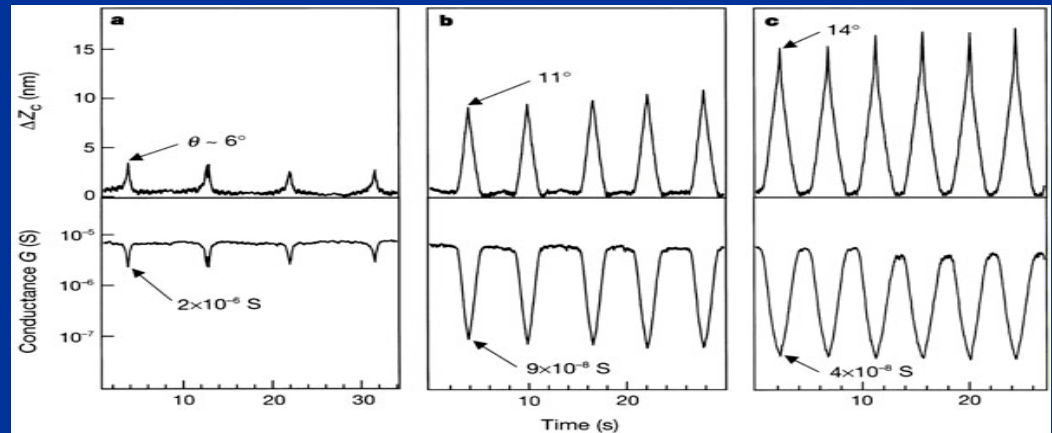
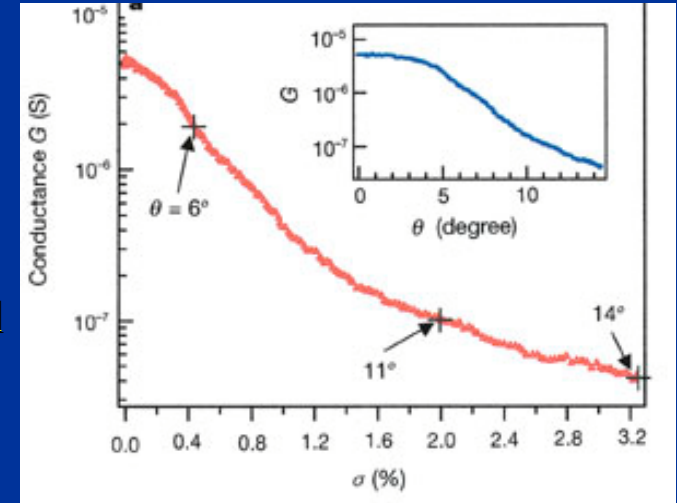
# Electromechanical action

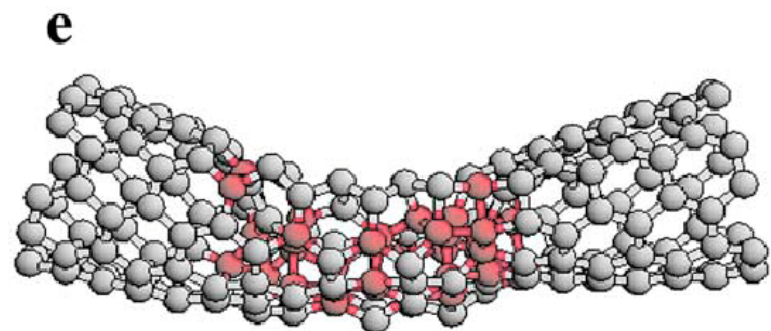
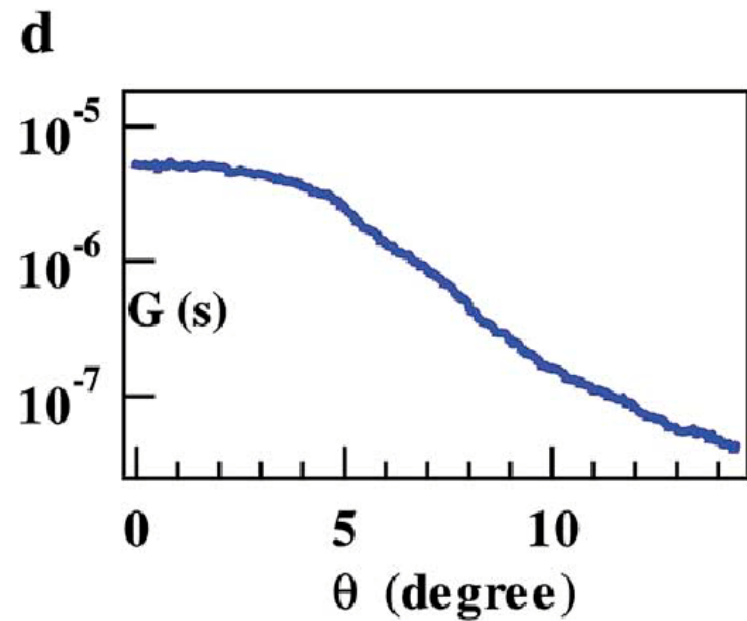
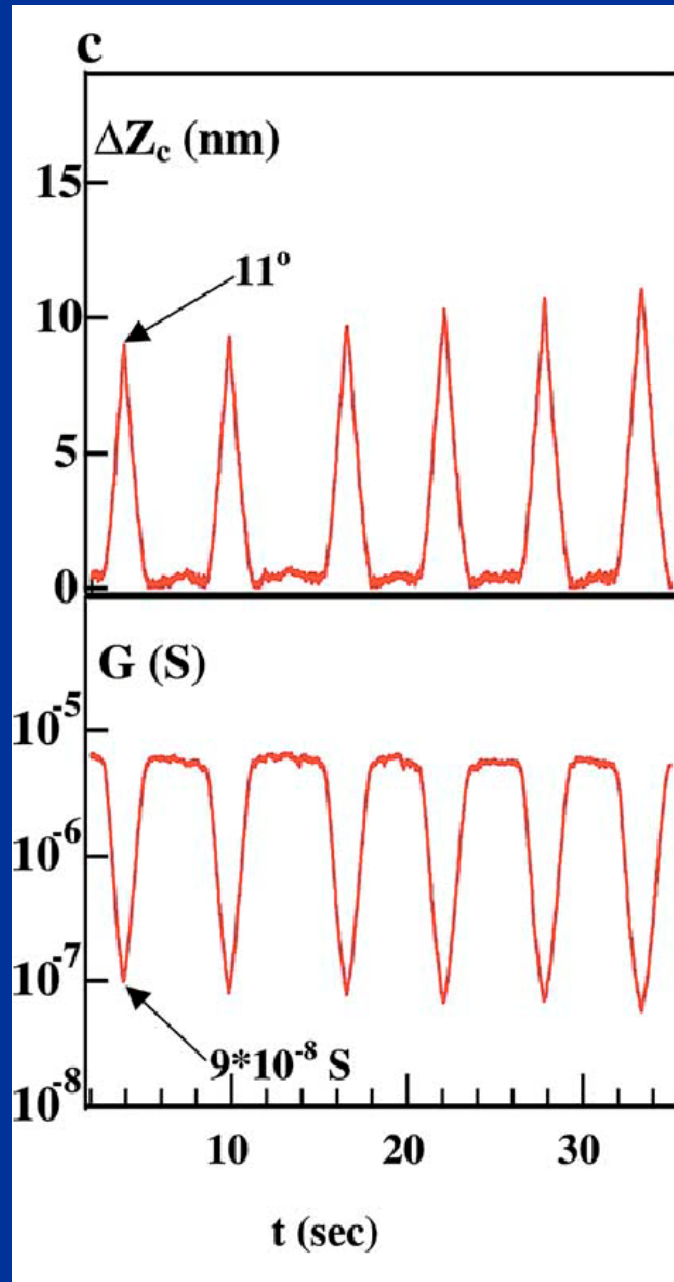
H.Dai (2000)



- Me-SWNT suspended length  $\sim 605$  nm,  $d \sim 3.1$  nm
- Trench  $\sim 500$  nm wide and  $\sim 175$  nm deep.
- $3-4 \mu\text{m}$  between metal electrodes: 20 nm Ti + 60 nm Au (on top)

Conductance is suppressed in phase with NT deflection. For maximum deflection it is  $10^{-2}$  modulation.

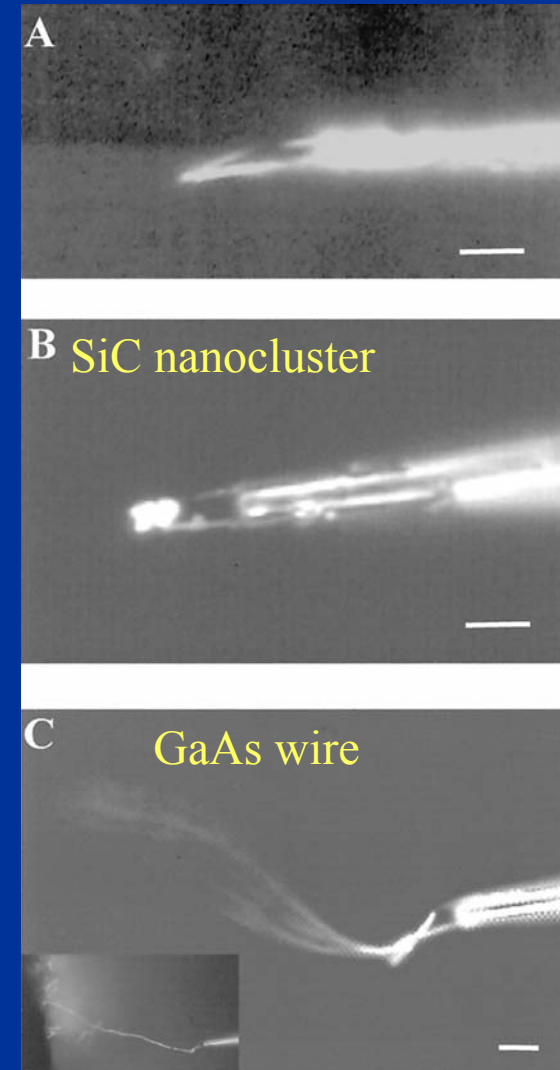
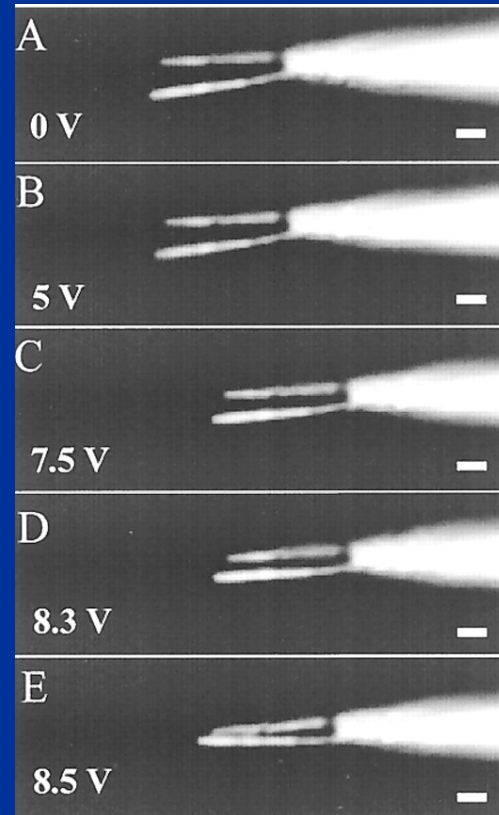
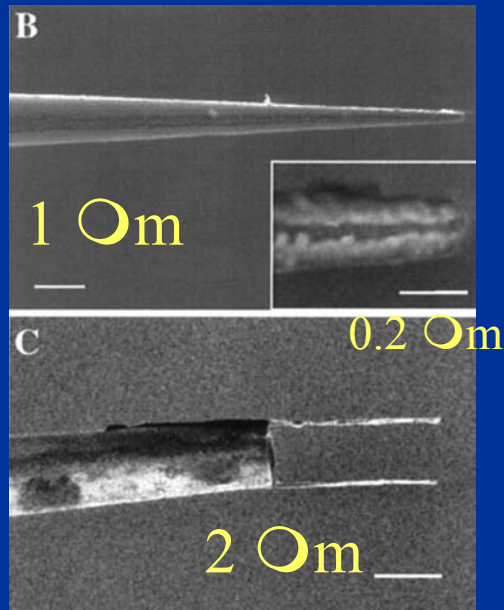
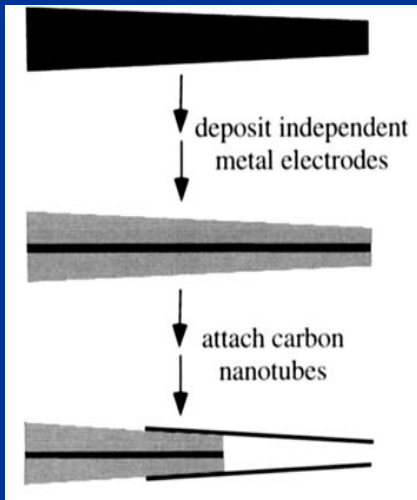




# Nanotube Tweezers

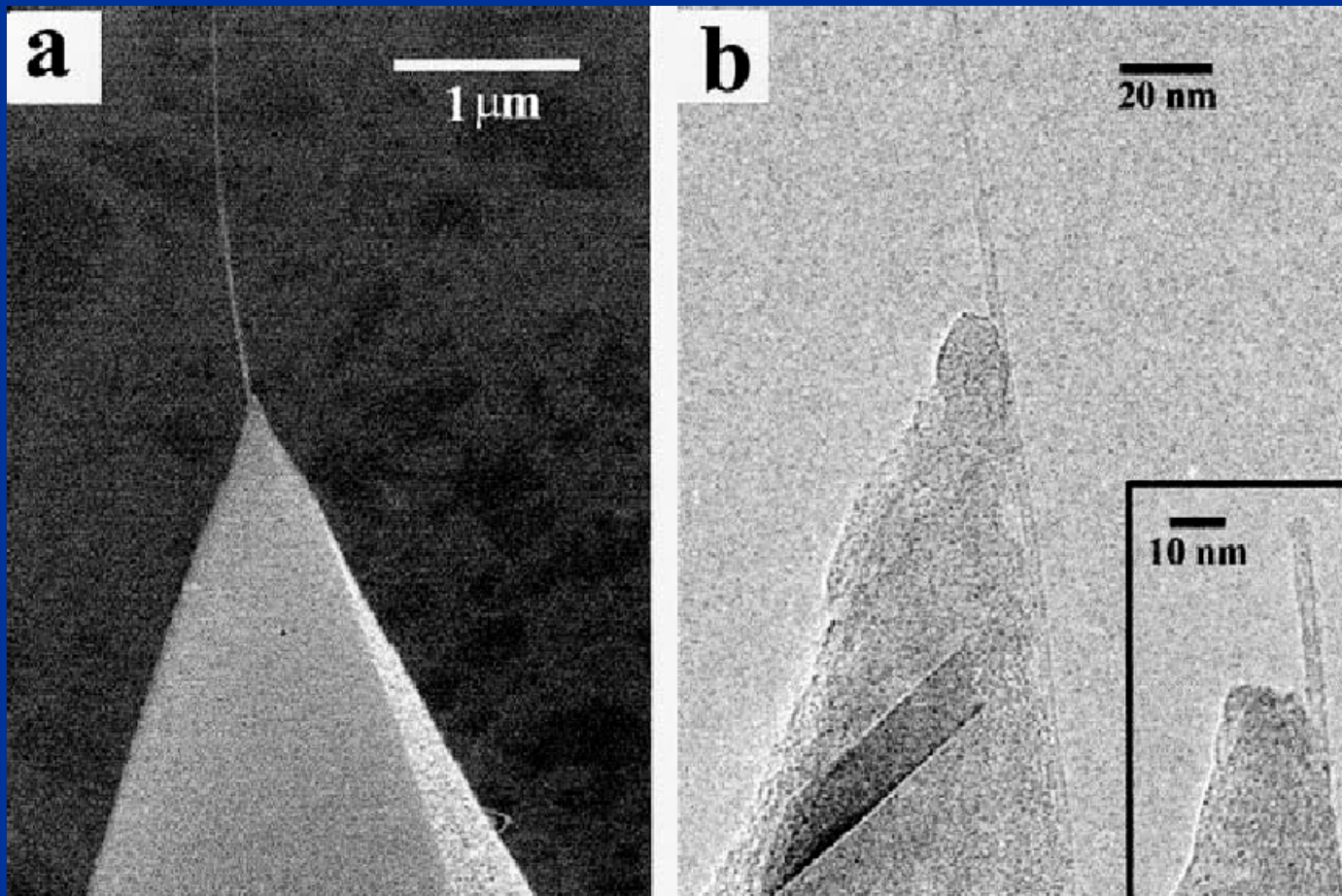
Ch.Lieber et.al., Science 1999

**Voltage up to 8.5 V  
controls tweezers closing  
Positive V can open NT-Tw**





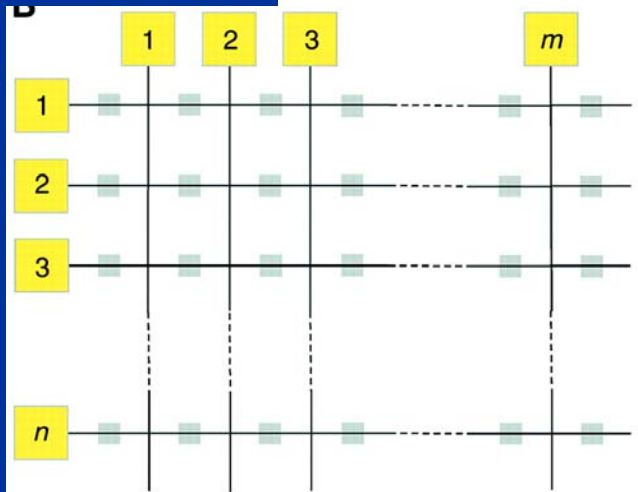
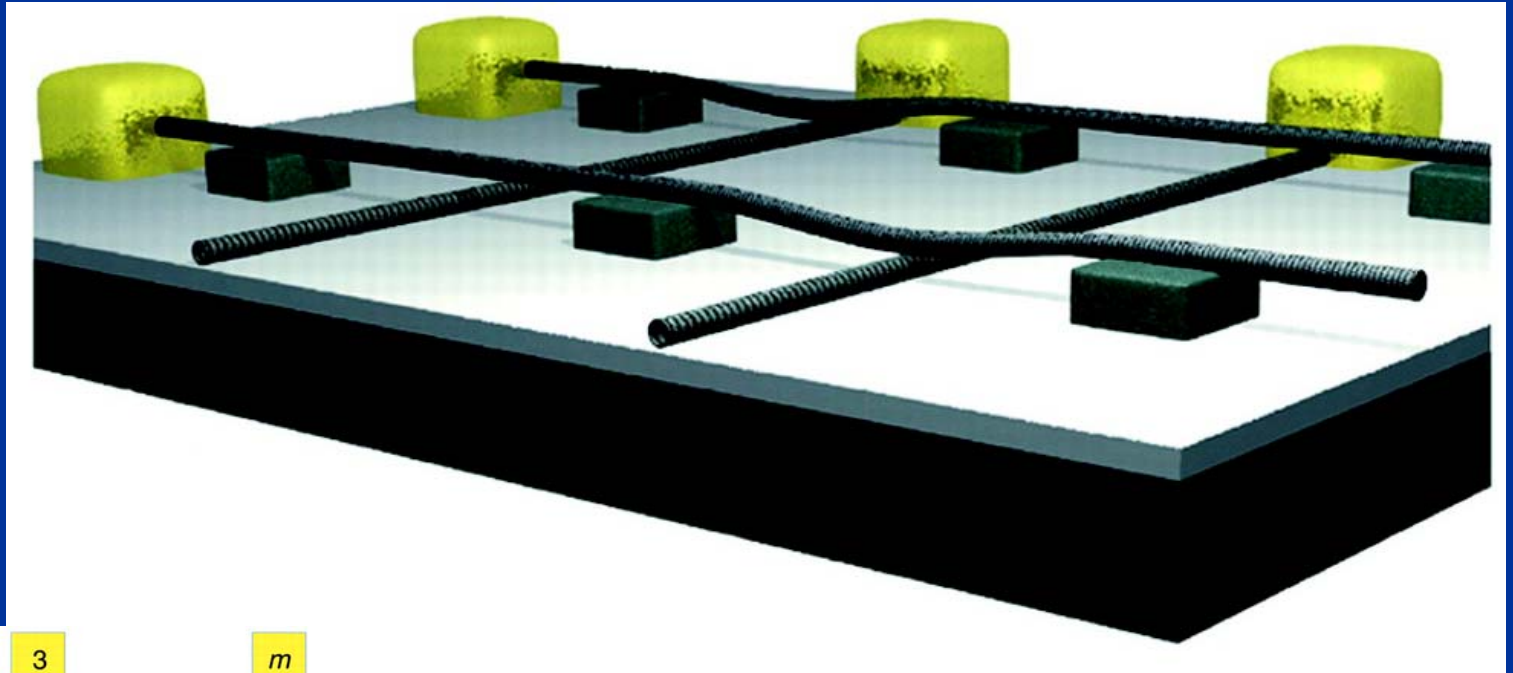
# Nanotube Tips



H.Dai et.al.

Ch.Lieber et.al.

# NT Memory Device



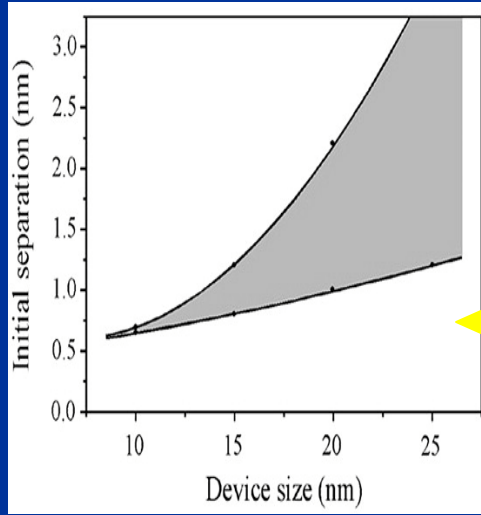
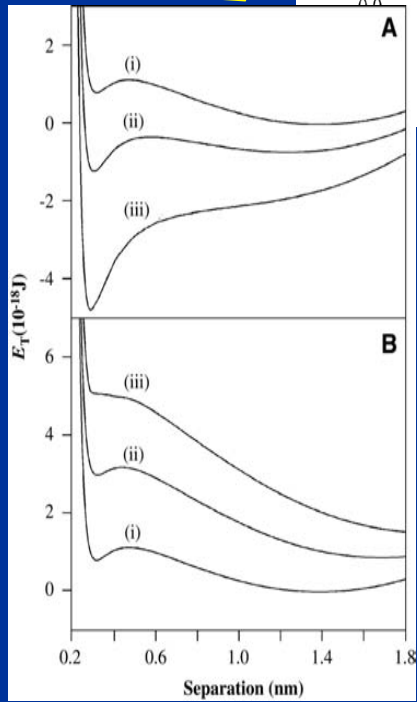
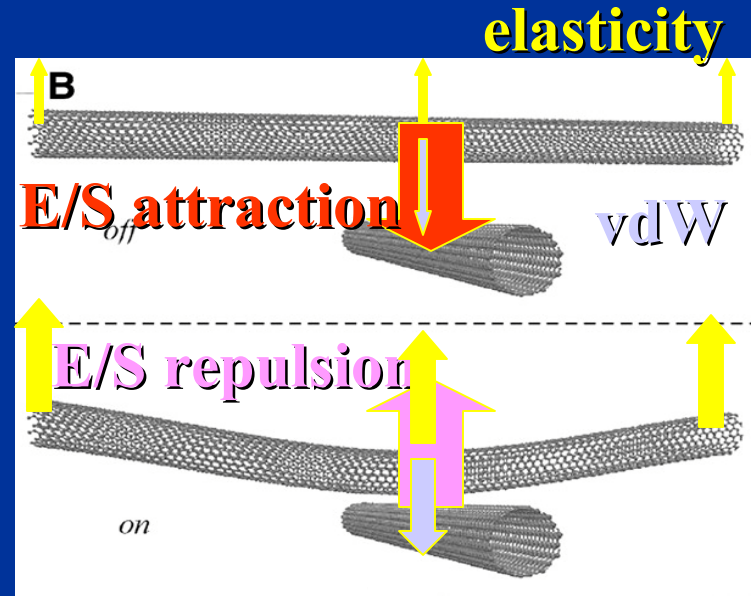
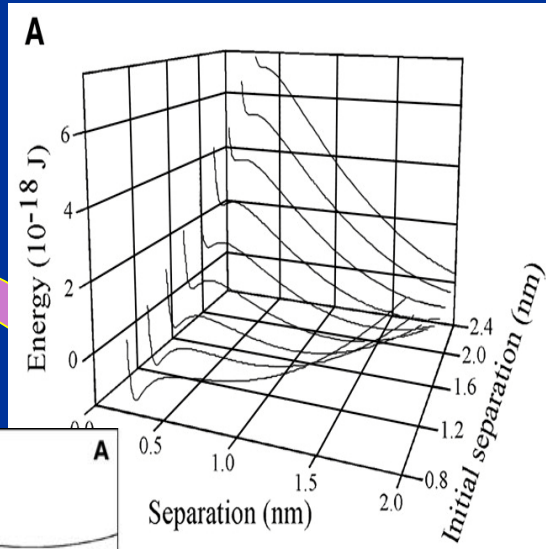
Ch.Lieber 2000

## Principles of operation

- upper rows suspend over bottom columns
- vdW attraction between wires (vs elastic module) shortens gap = better tunnel contact (ON state)
- negative bias can repulse wires (turns OFF state)
- positive bias switches back to ON

# NT Memory Device

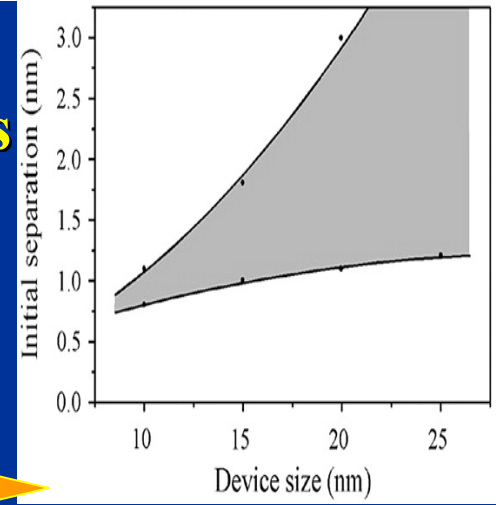
Ch.Lieber 2000



**Bistability region opens**

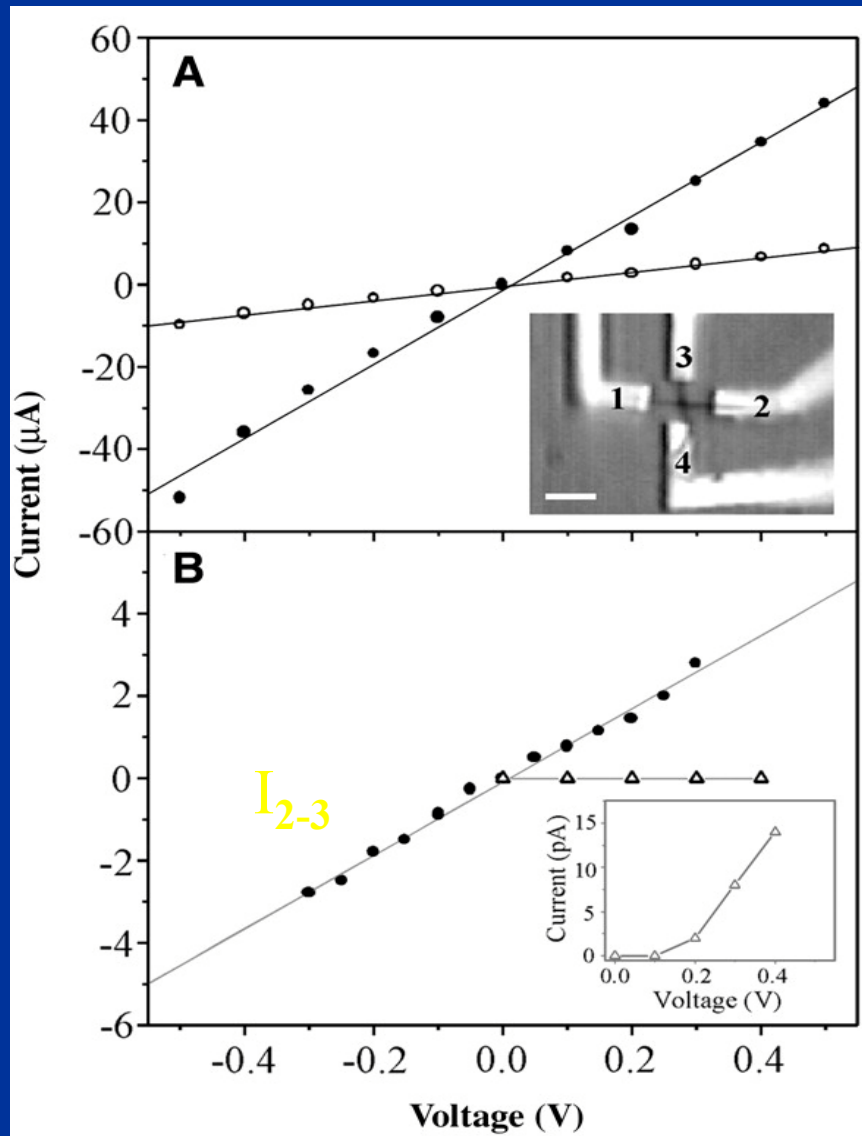
**Si support**

**softer organics**



# NT Memory Device

Ch.Lieber 2000

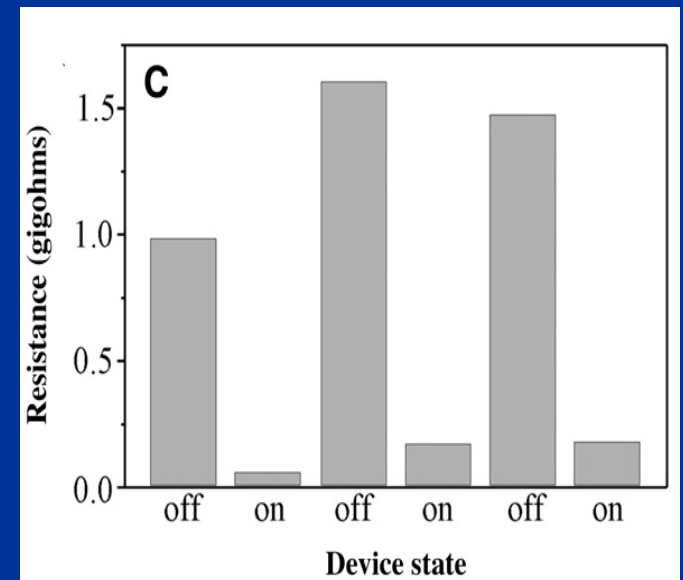


**First experimental manifestation**

$D_{\text{rope}} \sim 50\text{nm}$ ;  $L \sim 3\text{-}5\text{ }\mu\text{m}$ ,  $V_{\text{ON}} \sim 2.5\text{V}$

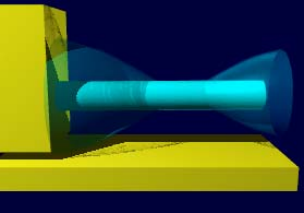
$R_{1-2} \sim 11\text{ k}\Omega$    $R_{3-4} \sim 58\text{ k}\Omega$  

$R_{\text{ON}} \sim 112\text{ k}\Omega$ ,  $R_{\text{OFF}} \sim 10\text{ G}\Omega$



**Reversible switching:  $V_{\text{ON}} \sim \pm 5\text{V}$ ,  $V_{\text{OFF}} \sim 40\text{V}$ .**

$R_{\text{OFF}} \sim 1.36\text{ G}\Omega$  and  $R_{\text{ON}} \sim 140\text{ M}\Omega$  



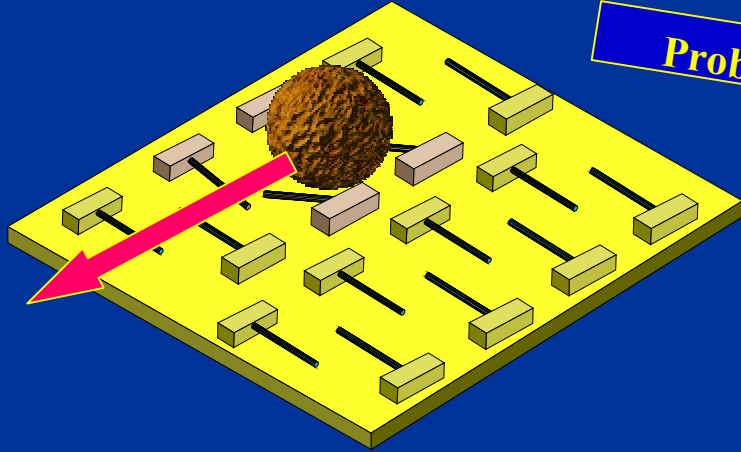
# Motivation

- **An advanced simulation of nano-scale systems becomes more and more challenging when approaches the nanosize from both sides: from the bulk, scaling down to nanostructures and from the atom side, scaling up to molecules.**
- **The complexity of the Quantum Mechanical calculation, which gives a full description, restricts its applicability to systems of limited size.**
- **Even if “There’s Plenty of Room at the Bottom”... we have to be able using it.**

R.Feinman 12/29/59

# NEMS: Simulation Hierarchy

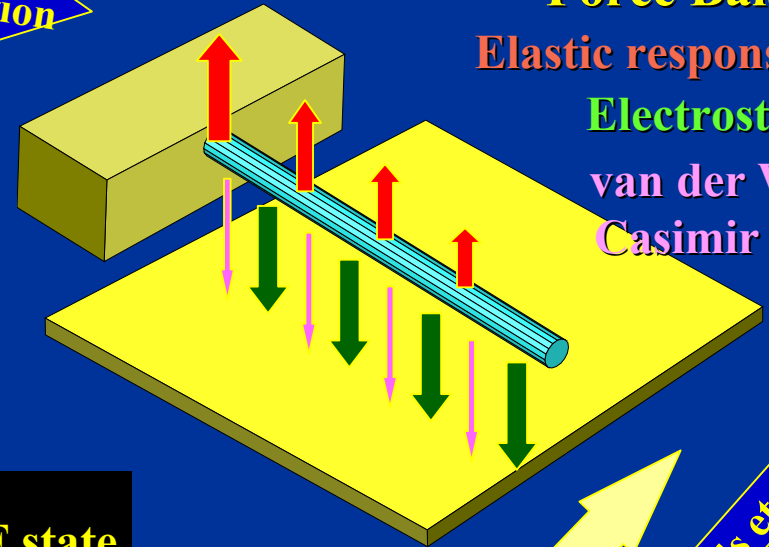
## A. System Level



Device optimization

Problem formulation

## B. Continuum Models

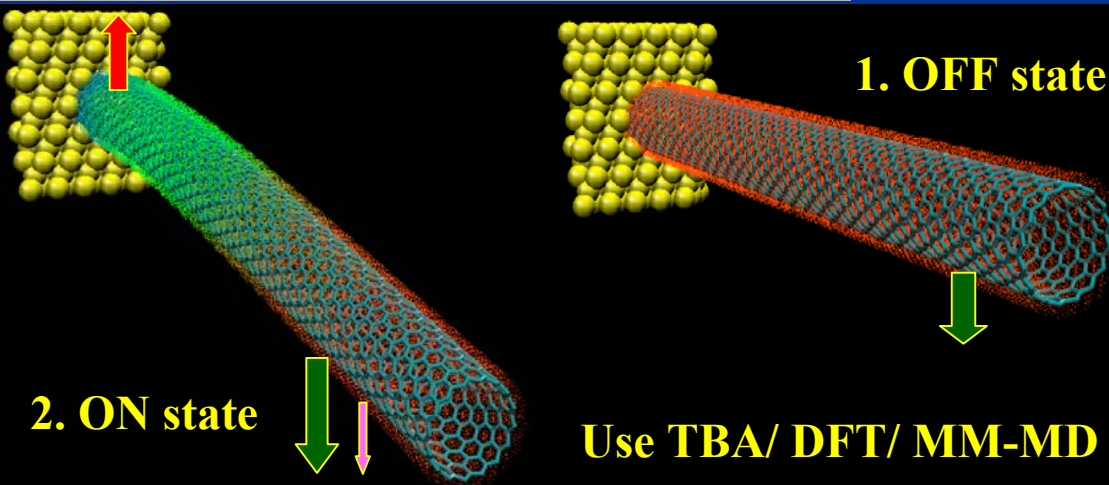


**Force Balance:**  
Elastic response vs.  
Electrostatics +  
van der Waals/  
Casimir forces

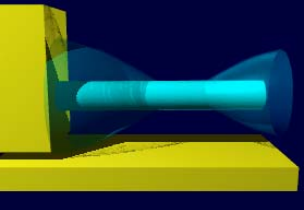
Energy parameters

Geometry, fields etc.

## C. Atomistic Level Simulation

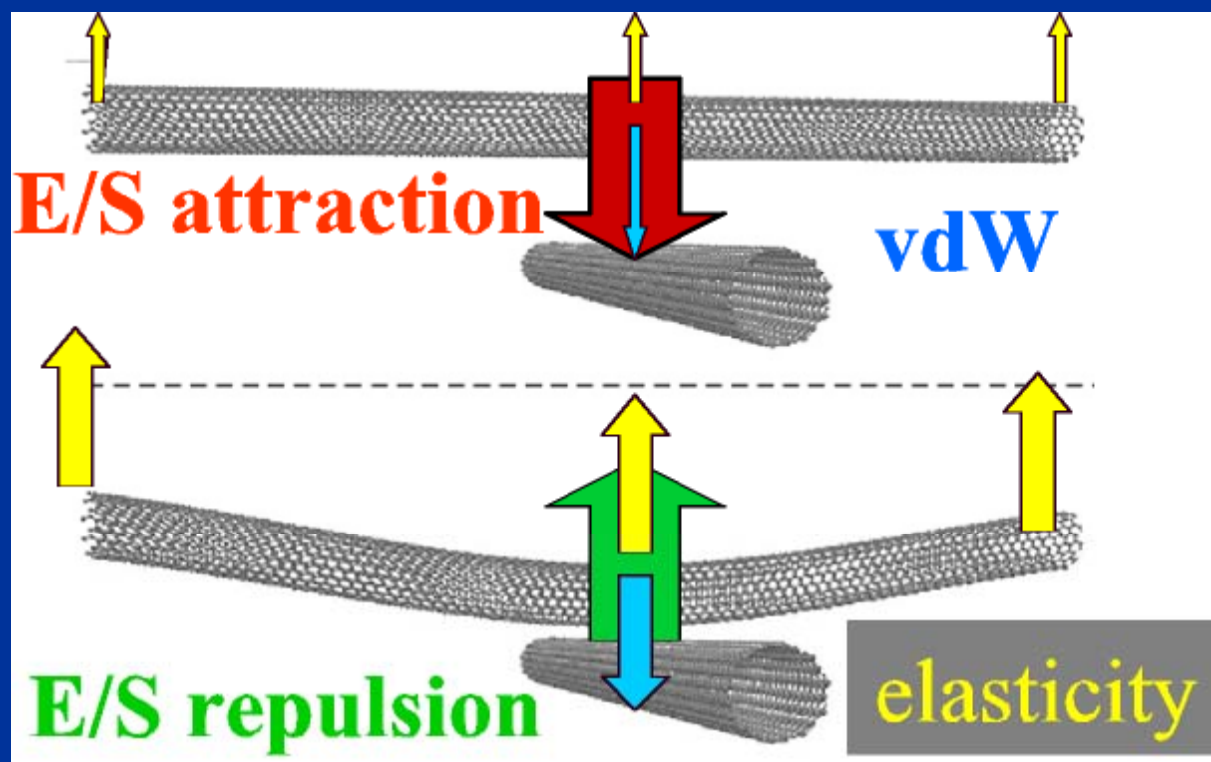


Use TBA/ DFT/ MM-MD (Quantum Mechanical Description)



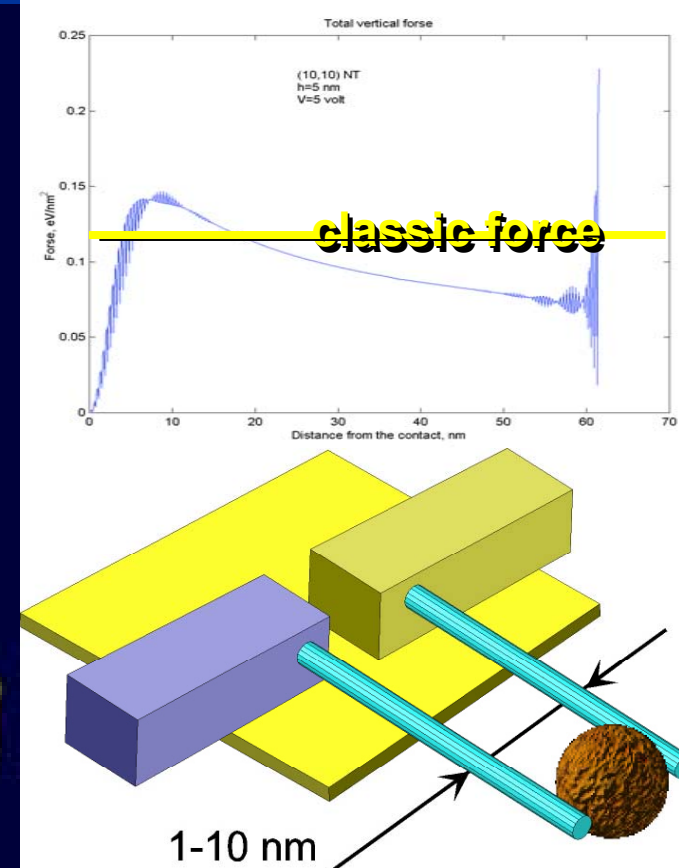
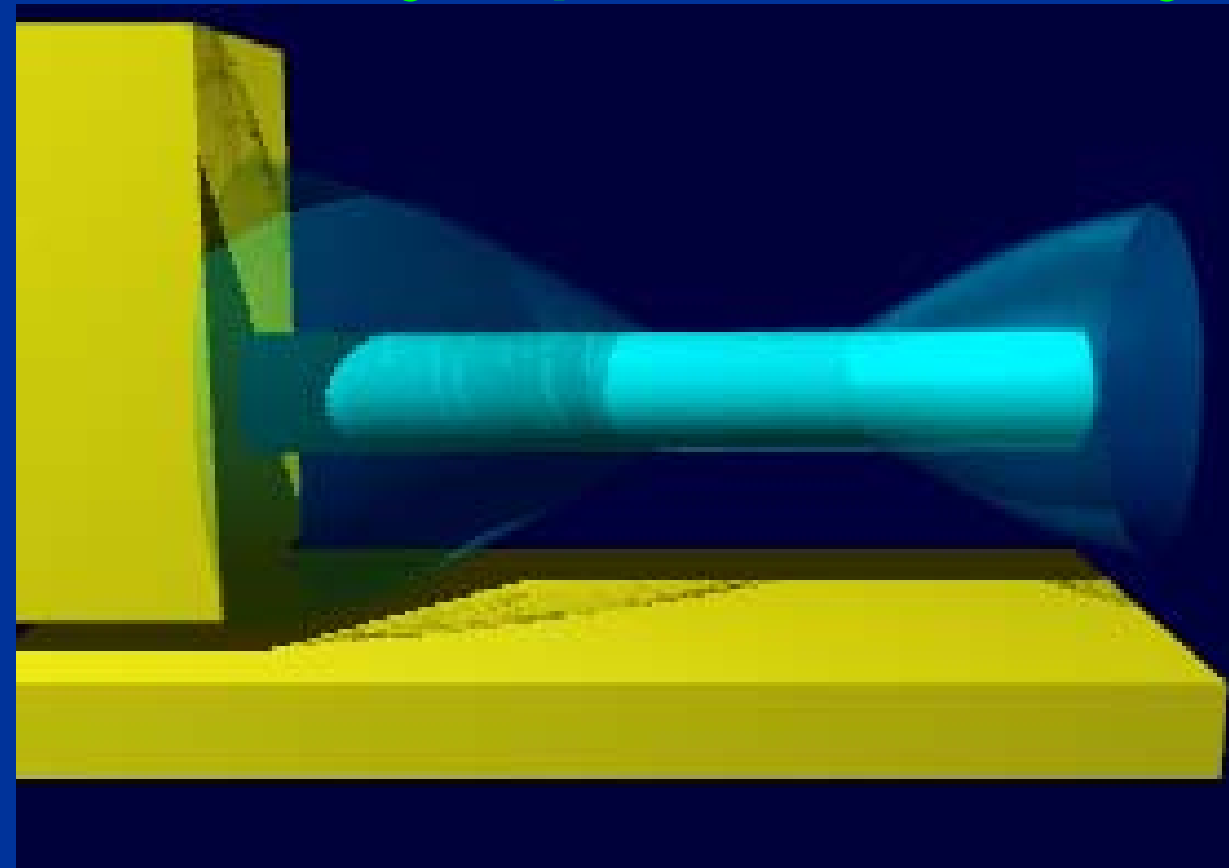
# Combine Continuum and Atomistic Models

- Fast and effective Device Simulation requires to develop a compact model which cannot be fully atomistic or continuum model but the combination



Ch.Lieber, Science (2000)

# Why special theory for NTDs?



- In contrast to micrometer scale devices, NT device models deviate from a classical description
- Fully Atomistic approach is precise but too complicated
- We develop a fast and accurate way of analytical description